iScience

CellPress
OPEN ACCESS

Article

BCL11B is positioned upstream of PLZF and RORγt to control thymic development of mucosal-associated invariant T cells and MAIT17 program

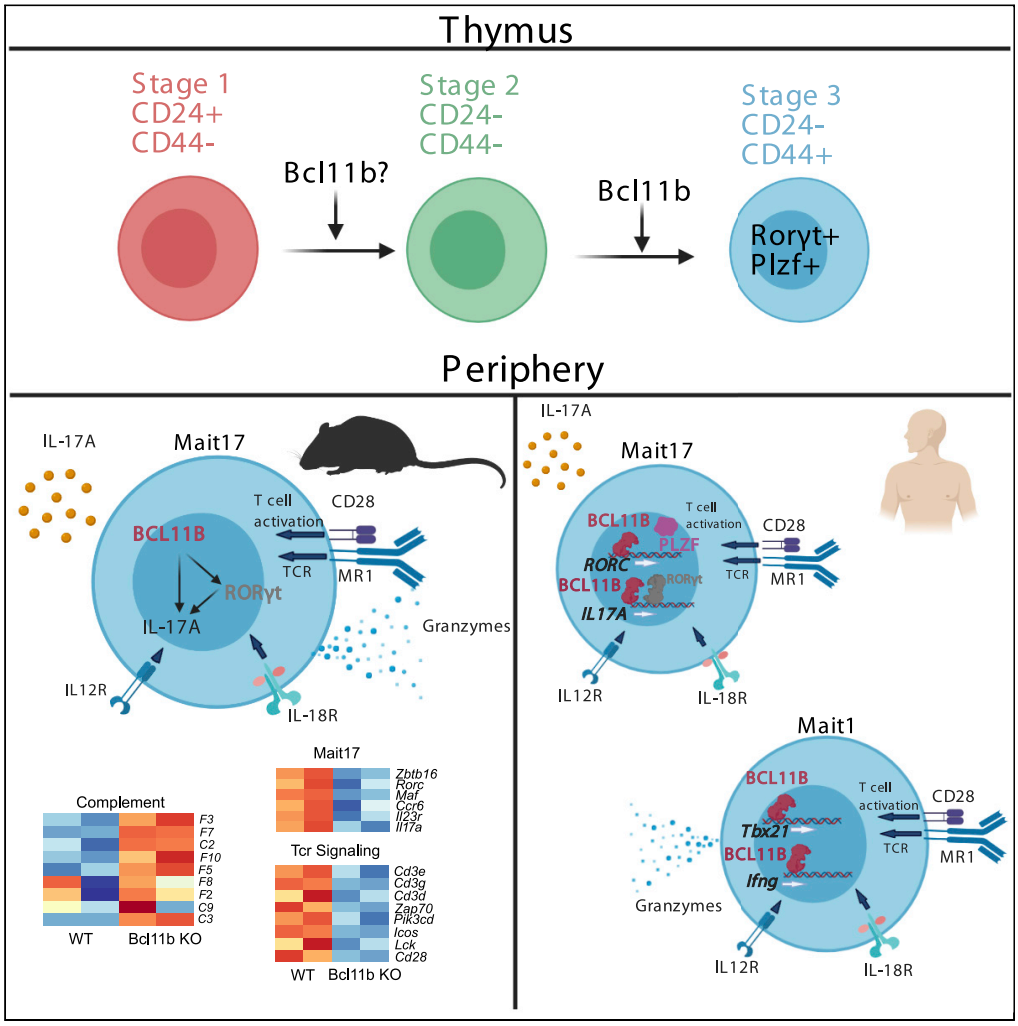

Theodore T. Drashansky, Eric Y. Helm, Nina Curkovic, ..., Weizhou Zhang, Liang Zhou, Dorina Avram

dorina.avram@moffitt.org

Highlights

BCL11B controls MAIT cell development in mice, predominantly MAIT17 lineage

BCL11B sustains MAIT17 and TCR signaling programs at steady state and in infection

BCL11B binds at MAIT17 and TCR program genes in human MAIT cells

Many BCL11B binding sites at MAIT17 and TCR genes are at putative active enhancers

Drashansky et al., iScience 24, 102307
April 23, 2021
https://doi.org/10.1016/j.isci.2021.102307

iScience

CellPress
OPEN ACCESS

Article

BCL11B is positioned upstream of PLZF and RORγt to control thymic development of mucosal-associated invariant T cells and MAIT17 program

Theodore T. Drashansky,[1,10] Eric Y. Helm,[1,10] Nina Curkovic,[1] Jaimee Cooper,[1] Pingyan Cheng,[2] Xianghong Chen,[2] Namrata Gautam,[2] Lingsong Meng,[3] Alexander J. Kwiatkowski,[4] William O. Collins,[5] Benjamin G. Keselowsky,[4] Derek Sant'Angelo,[6] Zhiguang Huo,[3] Weizhou Zhang,[7,8] Liang Zhou,[8,9] and Dorina Avram[1,2,8,11,*]

SUMMARY

Mucosal-associated invariant T (MAIT) cells recognize microbial riboflavin metabolites presented by MR1 and play role in immune responses to microbial infections and tumors. We report here that absence of the transcription factor (TF) Bcl11b in mice alters predominantly MAIT17 cells in the thymus and further in the lung, both at steady state and following *Salmonella* infection. Transcriptomics and ChIP-seq analyses show direct control of TCR signaling program and position BCL11B upstream of essential TFs of MAIT17 program, including RORγt, ZBTB16 (PLZF), and MAF. BCL11B binding at key MAIT17 and at TCR signaling program genes in human MAIT cells occurred mostly in regions enriched for H3K27Ac. Unexpectedly, in human MAIT cells, BCL11B also bound at MAIT1 program genes, at putative active enhancers, although this program was not affected in mouse MAIT cells in the absence of Bcl11b. These studies endorse BCL11B as an essential TF for MAIT cells both in mice and humans.

INTRODUCTION

Mucosal-associated invariant T (MAIT) cells reside at mucosal sites and respond to bacterial infections. They have an invariant TCRα chain paired with a TCRβ chain of limited diversity that recognizes riboflavin metabolites produced by bacteria and yeast and presented in the context of the evolutionary conserved MHC class I-like molecule MR1 (Tilloy et al., 1999; Treiner et al., 2003; Gold et al., 2010; Le Bourhis et al., 2010; Kjer-Nielsen et al., 2012; Corbett et al., 2014). MAIT cells are abundant in humans, including in peripheral blood, and are known to produce IL17 and IFNγ (Dusseaux et al., 2011; Le Bourhis et al., 2010; Gherardin et al., 2018). In common laboratory mice, MAIT cells are in reduced numbers and are predominantly Rorγt+ IL17-producing (MAIT17), while Tbet + MAIT1 cells are barely detectable (Koay et al. 2016, 2019; Godfrey et al., 2019; Rahimpour et al., 2015). MAIT cell precursors are selected by thymocytes which present riboflavin precursors in the context of MR1. Commensal bacteria producing riboflavin metabolites are necessary for their development, and numbers of MAIT cells are much lower in germ free mice (Koay et al., 2016; Martin et al., 2009; Constantinides et al., 2019; Legoux et al., 2019a). MAIT cell development in the thymus consists of three sequential stages: stage 1 (CD24 + CD44-), stage 2 (CD24-CD44-), and stage 3 (CD24-CD44+) (Koay et al. 2016, 2019). Several transcription factors (TFs) have been found essential for MAIT cell development and function. Absence of the TF Tcf7, expressed early in thymic MAIT cells and downregulated at stage 3 (Koay et al., 2019), causes a major deficiency in MAIT cells (Mielke et al., 2019), and so does Bcl6 (Gioulbasani et al., 2020). The TF Zbtb16 (PLZF) reaches the highest levels at stage 3, remaining elevated mostly in MAIT17 cells in common laboratory C57B6/L mice (Koay et al., 2019), different from iNKT cells where PLZF is expressed very early and then downregulated in mature iNKT cells, with the exception of iNKT2 cells (Kovalovsky et al., 2008; Savage et al., 2008; Lee et al., 2013). A recent study using Cast/C57BL/6 mice, which have increased iVα19 -Jα33 rearrangements and thus elevated numbers of MAIT cells (Cui et al., 2015), proposed that SAP signaling initiated by selection mediated by DP thymocytes promotes expression of PLZF, which remains expressed in both MAIT1 and MAIT17 cells, albeit at higher levels in MAIT17 (Legoux et al., 2019b). The same study showed that Cast/C57BL/6 mice have, in addition to the CD44+ PLZF+ MR1t-5-OP-RU+ MAIT cells, a population of MR1t-5-OP-RU+ cells

[1]Department of Anatomy and Cell Biology, College of Medicine, University of Florida, Gainesville, FL 32610, USA

[2]Department of Immunology, H. Lee Moffitt Cancer Center and Research Institute, 12902 Magnolia Dr, Tampa, FL 33612, USA

[3]Department of Biostatistics, College of Medicine, College of Public Health & Health Professions, University of Florida, Gainesville, FL 32611, USA

[4]J. Crayton Pruitt Family Department of Biomedical Engineering, University of Florida, Gainesville, FL 32611, USA

[5]Department of Otolaryngology, College of Medicine, University of Florida, Gainesville, FL 32605, USA

[6]Department of Pediatrics, The Child Health Institute of NJ, Robert Wood Johnson Medical School, New Brunswick, NJ 08903, USA

[7]Department of Pathology, Immunology and Laboratory Medicine, College of Medicine, University of Florida, Gainesville, FL 32610, USA

[8]UF Health Cancer Center, Gainesville, FL 32610, USA

[9]Department of Infectious Diseases and Immunology, College of Veterinary Medicine, University of Florida, Gainesville, FL 32608, USA

[10]These authors contributed equally

[11]Lead contact

*Correspondence: dorina.avram@moffitt.org

https://doi.org/10.1016/j.isci.2021.102307

selected on thymic epithelial cells, which do not express PLZF and have a naive phenotype (Legoux et al., 2019b), similar to the transgenic mice with TRAV1 TRAJ33 (reviewed in (Godfrey et al., 2019)). It is unclear if such MR1t-5-OP-RU+ cells selected on thymic epithelial cells exist in NON-Cast/C57BL/6 mice.

In common laboratory C57BL/6 mice, stage 3 MAIT cells comprise mostly RORγt+ MAIT17 cells (Rahimpour et al., 2015; Koay et al. 2016, 2019). The essential role of RORγt in MAIT cells is supported by the fact that biallelic *RORC* functional loss in humans results in absence of MAIT cells (Okada et al., 2015). RORγt is essential for MAIT17 program, including in controlling expression of IL17A at steady state and in infection (Dusseaux et al., 2011; Koay et al. 2016, 2019; Chen et al., 2017). Another TF, c-Maf, also upregulated at stage 3, is part of the MAIT17 signature (Koay et al., 2019). Although MAIT1 population is scarce in mice at steady state, following bacterial infection, when MAIT cells expand, Tbet is upregulated and a considerable number of MAIT cells become Rorγt+ Tbet+ (Wang et al., 2019; Chen et al., 2017). In humans, MAIT cells respond to viral infection by producing IFNγ and granzyme B (Gzmb) to lyse infected cells (Le Bourhis et al., 2013; van Wilgenburg et al. 2016, 2018; Kurioka et al., 2015; Sattler et al., 2015; Slichter et al., 2016; Ussher et al., 2014).

MAIT cells have been also suggested to play a role in tumor immunity, responding by cytotoxic activity to myeloma cells loaded with 5-OP-RU (Gherardin et al., 2018). However, a reduction of these cells was observed in peripheral blood of patients with mucosal tumors and an accumulation in tumors, and not always with a favorable outcome (reviewed in (Godfrey et al., 2019; Vacchini et al., 2020)).

Bcl11b is a TF expressed in all T cells and innate lymphoid cells. It plays a fundamental role in T cell lineage commitment in mice and humans (Li, Leid and Rothenberg 2010a; Li et al., 2010b; Garcia-Perez et al., 2020; Roels et al., 2020; Dolens et al., 2020), and in beta and positive selection and survival of thymocytes (Wakabayashi et al., 2003; Albu et al., 2007; Avram and Califano 2014). Bcl11b is essential for development of CD4+ and CD8+ T cells (Albu et al., 2007; Kastner et al., 2010; Kojo et al., 2017), as well as of Treg cells (Vanvalkenburgh et al., 2011; Drashansky et al., 2019; Hasan et al., 2019) and iNKT cells (Albu et al., 2011; Kastner et al., 2010; Uddin et al., 2016). Absence of Bcl11b in DP thymocytes results in lack of iNKT cells due to Bcl11b's role in the control of glycolipid processing and presentation by thymocytes, as well as intrinsic alterations in iNKT cell precursors (Albu et al., 2011). Specific ablation of Bcl11b in iNKT cells results in reduction of iNKT1 and iNKT2 subsets and increased expression of iNKT17 program genes (Uddin et al., 2016). Bcl11b also controls the function of mature effector CD4+ T cells and their identity (Fang et al., 2018; Califano et al., 2014; Lorentsen et al., 2018), as well as Ag-specific expansion of CD8+ T cells (Zhang et al., 2010; Abboud et al., 2016). Thus, in addition to a common essential function of Bcl11b in maintaining T cell identity, Bcl11b plays specific and complex roles in each of the T cell lineages and subsets. In addition to T cells, Bcl11b is essential for ILC2 development and identity maintenance and function (Califano et al., 2015; Walker et al., 2015; Yu et al., 2015) and NK cell immunity (Holmes et al., 2021). In this study, we show an essential intrinsic role of Bcl11b in MAIT cell development and function. Transcriptomics analysis revealed major alterations in the MAIT17 program, CD3 and TCR signaling and cytotoxic granule exocytosis (CGE) programs, but not in MAIT1 program in murine Bcl11b KO MAIT cells. BCL11B and H3K27Ac ChIP-seq analyses in human MAIT cells revealed binding of BCL11B at key genes of the MAIT17 program, many of them associated with putative active enhancers. BCL11B also bound at CD3 complex and at essential genes of TCR signaling program, and surprisingly at MAIT1 program genes in regions with enriched H3K27Ac. Many of the human genes where BCL11B bound are the homologs of the mouse genes regulated by Bcl11b, with the exception of MAIT1 genes, which were not found dysregulated in mouse MAIT cells by absence of Bcl11b. This study thus demonstrates an essential role of Bcl11b in the development of MAIT cells and in the control of MAIT17 cell program at steady state and in infection and positions Bcl11b in the context of critical TFs that regulate these cells. The role of Bcl11b in positively supporting MAIT17 program is in contrast to its role in iNKT cells, where Bcl11b was required to sustain iNKT1 and iNKT2 programs, but restrained the iNKT17 program (Uddin et al., 2016), further supporting the concept that Bcl11b, in addition to regulating common programs in T cells, exerts also complex lineage and subset specific roles.

RESULTS

Bcl11b is essential for MAIT cell development and MAIT17 subset

Bcl11b is expressed in all αβ T cell populations that derive at the DP stage of T cell development (Albu et al. 2007, 2011; Zhang et al., 2010; Lorentsen et al., 2018; Drashansky et al., 2019; Fang et al., 2018; Hasan et al., 2019; Vanvalkenburgh et al., 2011). Considering that MAIT cells are also generated at this stage, we evaluated Bcl11b in thymic and peripheral MAIT cells and found it expressed at an equivalent level throughout

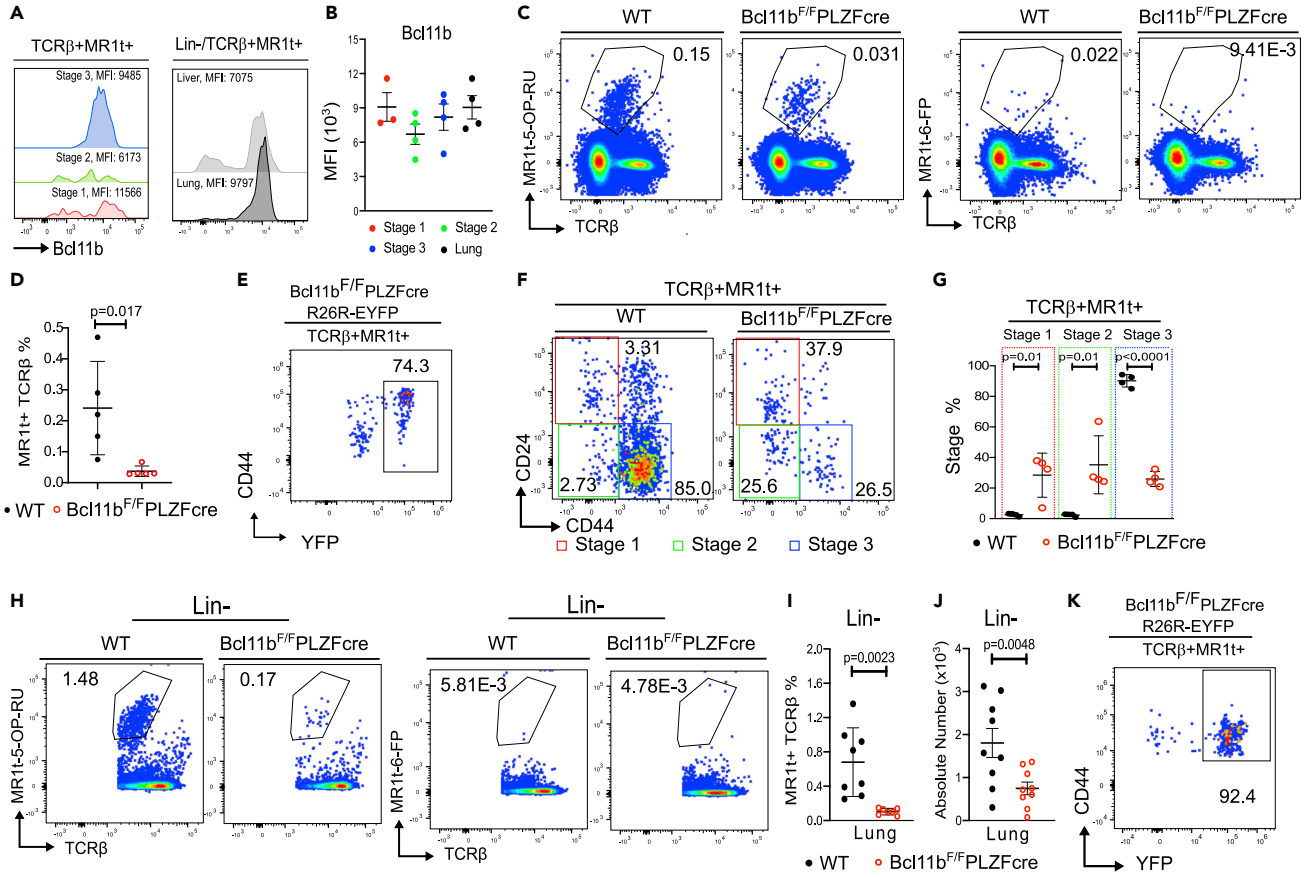

Figure 1. MAIT cells in the thymus and lung in the absence of Bcl11b at steady state

(A) Representative histograms of Bcl11b in TCRβ+MR1t-5-OP-RU+ MAIT cells. Thymic developmental stages (left), liver and lung (right).

(B) Bcl11b MFI in MAIT cells in thymic developmental stages and lung (n = 4).

(C) Representative dot plots of MR1t-5-OP-RU and control MR1t-6-FP staining in thymi of Bcl11b$^{F/F}$/PLZFcre and Bcl11b$^{F/F}$ (WT) mice.

(D) Frequencies of TCRβ+MR1t-5-OP-RU+ MAIT cells from thymi of Bcl11b$^{F/F}$/PLZFcre and Bcl11b$^{F/F}$ (WT) mice (n = 5). The data from thymus are derived from 10 pairs of mice in which two FACS files from the same type of mice (KO or WT) were concatenated.

(E) Representative dot plot of YFP and CD44 in TCRβ+MR1t-5-OP-RU+ MAIT cells isolated from thymi of Bcl11b$^{F/F}$/PLZFcre/R26R-EYFP mice.

(F and G) Representative dot plots (F) and frequencies (G) of Bcl11b KO and WT TCRβ+MR1t-5-OP-RU+ MAIT cell developmental stages in thymi of Bcl11b$^{F/F}$/PLZFcre and WT mice (n = 4). The data are derived from 8 pairs of mice in which two FACS files from the same type of mice (KO or WT) were concatenated.

(H) Representative dot plots of MR1t-5-OP-RU and control MR1t-6-FP staining in lung of BCL11B$^{F/F}$/PLZFcre and BCL11B$^{F/F}$ (WT) mice.

(I and J) Frequencies (I) and absolute numbers (J) of TCRβ+MR1t-5-OP-RU+ MAIT cells in lung of Bcl11b$^{F/F}$/PLZFcre and WT mice. Each dot represents the data from one mouse.

(K) Representative dot plot of YFP and CD44 in TCRβ+MR1t-5-OP-RU+ MAIT cells isolated from the lung of Bcl11b$^{F/F}$/PLZFcre/R26R-EYFP mice at steady state.

Data are represented as mean ± SEM. Student's t-test was used for statistical analysis. $p < 0.05$ was considered significant.

all MAIT cell developmental stages, as well as in the lung MAIT cells (Figures 1A and 1B). The TF PLZF is known to be expressed in MAIT cells and iNKT cells, but not in DP thymocytes or other αβ T cell populations (Kovalovsky et al., 2008; Savage et al., 2008). We thus made use of Bcl11b$^{F/F}$/PLZFcre mice (Zhang et al., 2015) to study the role of Bcl11b in MAIT cells. Results show that Bcl11b$^{F/F}$/PLZFcre mice (non-Cast/C57BL/6) had a marked reduction in the thymic TCRβ+MR1t-5-OP-RU+ MAIT cells compared to WT (Figures 1C and 1D). The small number of TCRβ+MR1t-5-OP-RU+ cells in the thymus of Bcl11b$^{F/F}$/PLZFcre/R26R-EYFP mice were largely YFP+ (Figure 1E), demonstrating that they are dependent on PLZF expression, and thus not mainstream T cells.

Analysis of thymic developmental stages revealed a severe decrease of MAIT cell stage 3 frequency in Bcl11b$^{F/F}$/PLZFcre thymi compared to WT (Figures 1F and 1G). Further evaluation of TCRβ+MR1t-5-OP-

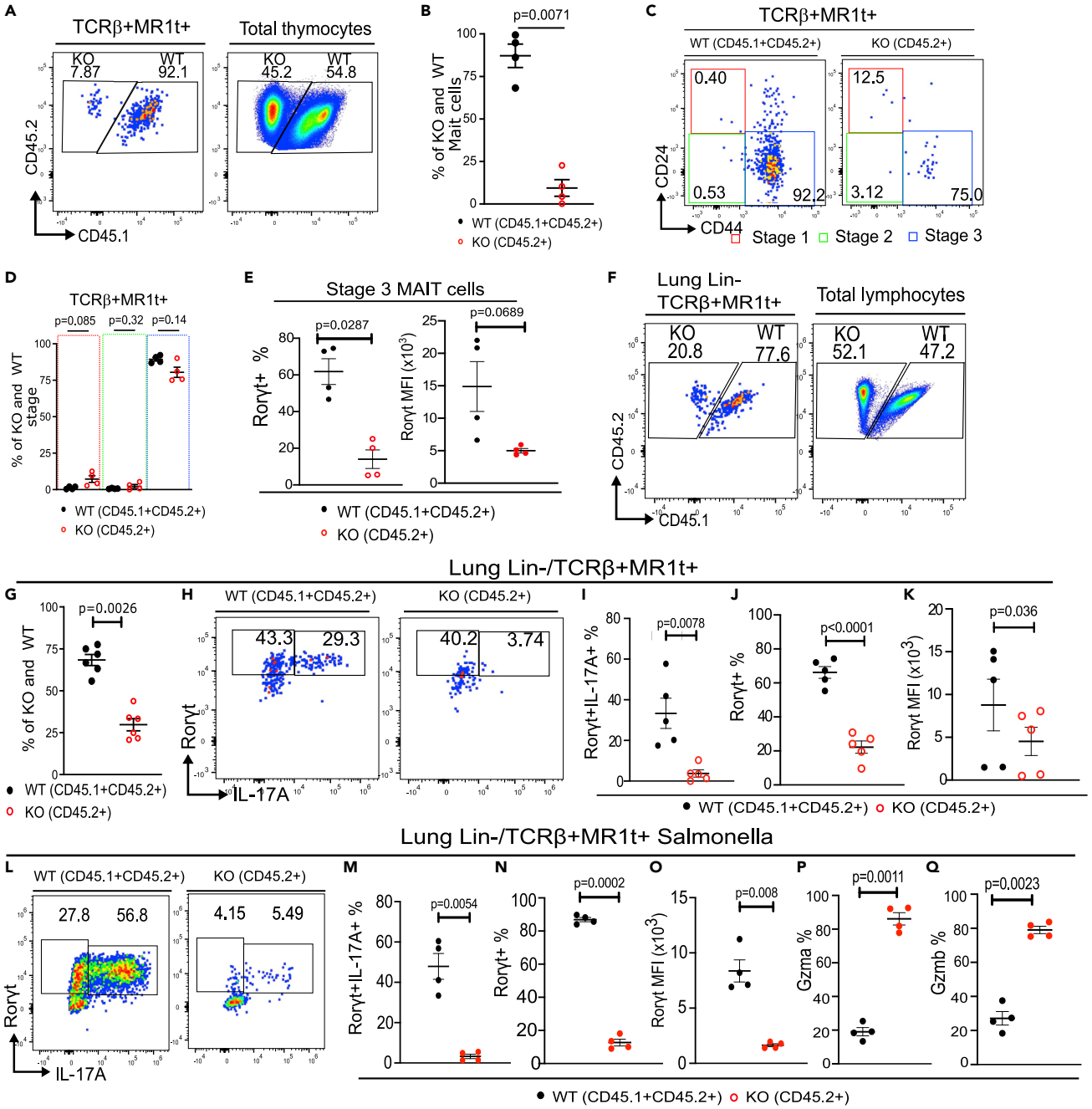

Figure 2. Defects in MAIT cells in the absence of Bcl11b are cell intrinsic

Mixed bone marrow (BM) chimeras were generated by 1:1 ratio of BM cells from Bcl11b$^{F/F}$/PLZFcre (KO) (CD45.2+) mice and Bcl11b$^{F/F}$ (WT) (CD45.1+ CD45.2+) mice, transplanted into lethally irradiated CD45.1 mice.

(A and B) Representative dot plot (A) and frequencies (B) of TCRβ+MR1t-5-OP-RU+ MAIT cells in the thymus, 8 weeks post transfer versus total transplanted thymocytes.

(C and D) Representative dot plot (C) and frequencies (D) of Bcl11b KO (CD45.2) and WT (CD45.1+ CD45.2+) TCRβ+MR1t-5-OP-RU+ MAIT cells in the three developmental stages in thymi of mixed BM chimeras.

(E) Frequencies and MFI of RORγt in developmental stage 3.

(F and G) Representative dot plots (F) and frequencies (G) of transplanted Bcl11b KO (CD45.2) and WT (CD45.1+ CD45.2+) TCRβ+MR1t-5-OP-RU+ MAIT cells versus TCRβ+MR1t-5-OP-RU- cells in the lung of mixed BM chimeric mice.

(H–K) Representative contour plots (H) and frequencies (I) of RORγt and IL17A, frequencies (J) and MFI (K) of RORγt in the lung Bcl11b KO (CD45.2) and WT (CD45.1+ CD45.2+) TCRβ+MR1t-5-OP-RU+ MAIT cells in transplanted BM chimeric mice at steady state.

Figure 2. *Continued*

(L–Q) Representative contour plots (L) and frequencies (M) of RORγt and IL17A, frequencies (N) and MFI (O) of RORγt, and Gzma (P) and Gzmb (Q) frequencies in the lung Bcl11b KO (CD45.2) and WT (CD45.1+ CD45.2+) TCRβ+MR1t-5-OP-RU+ MAIT cells in transplanted BM chimeric mice infected with 10^6 cfu of *Salmonella enterica* ser. Typhimurium BRD509 (*Salmonella* BRD509) intranasally. Two mouse files were concatenated using FlowJo for each point on the statistical graphs.

Data are represented as mean ± SEM. All statistics were conducted as paired t test. $p < 0.05$ was considered significant.

RU+ MAIT cells in the lung, where they are known to localize (Rahimpour et al., 2015; Salou et al., 2019), showed that their frequency and absolute numbers were further reduced in the absence of Bcl11b (Figures 1H–1J). The small number of TCRβ+MR1t-5-OP-RU+ CD44+ MAIT cells in the lung of Bcl11b$^{F/F}$/PLZFcre/R26R-EYFP mice were over 90% YFP+ (Figure 1K), demonstrating again that they are dependent on PLZF expression. Importantly, TCRβ+ MR1t-5-OP-RU+ PLZF-Cre-YFP+ were all CD44 positive at steady state (Figure 1K), and thus not main-stream T cells, which are known to be CD44 negative.

Mixed bone marrow chimeras (1:1, Bcl11b$^{F/F}$/PLZFcre:WT) further showed reduction of the Bcl11b KO TCRβ+MR1t-5-OP-RU+ MAIT cell frequency both in the thymus and in the lung (Figures 2A, 2B, 2F, and G), however the frequency of thymic developmental stage 3 was in large restored (Figures 2C and 2D). These results demonstrate that the numerical reduction is cell intrinsic, however cell extrinsic factors may contribute to the developmental defects. We previously showed that Bcl11b$^{F/F}$/PLZFcre mice had also reduced numbers of iNKT cells, with a major reduction in iNKT1 and iNKT2 subsets and reduced production of IL4 and IFNγ, including in the thymus (Uddin et al., 2016). Importantly, IL4Ra is expressed on thymic MAIT cells, being downregulated from early developmental stages to mature thymic MAIT cells (Koay et al., 2019). Thus, the reduction in IL4 in the thymus of Bcl11b$^{F/F}$/PLZFcre mice may negatively impact the transition of Bcl11b KO MAIT cells to mature stage 3, while in chimeric mice, when IL4 was provided by wild type iNKT2 cells, the transition of Bcl11b KO MAIT cells to stage 3 was largely restored, however not the reduced frequency of Bcl11b KO MAIT cells. Of note, IL4Ra was normally expressed by Bcl11b KO MAIT cells (Figure S1).

At thymic stage 3, two functional MAIT cell subsets have been identified, namely MAIT17, known to express Rorγt and numerically predominant in common lab C57BL/6 mice, and MAIT1, expressing Tbet and much lower numerically (Koay et al. 2016, 2019) (and Figures 3A and 3B). The Rorγt+ population was significantly decreased in stage 3 Bcl11b KO MAIT cells, however without resulting in an increase in the Tbet+ population, but rather in a population negative for both TFs (Figures 3A and 3B).

In the lung at steady state, as expected the Rorγt+ MAIT17 population was predominant, with barely detectable Tbet+ MAIT1 cells, and around 30% of MAIT cells negative for both Rorγt and Tbet (Figures 3C and 3D). Bcl11b KO Rorγt+ MAIT17 cell frequency was even more markedly diminished in the lung, representing only approximately 10% of that of WT. There was no increase in the Bcl11b KO Tbet+ MAIT1 population, but rather in the Rorγt-Tbet- MAIT cells, which represented over 90% (Figures 3C and 3D). Of note, Bcl11b levels were slightly but significantly higher in MAIT17 cells in the thymus and lung of WT mice compared to both MAIT1 and Rorγt-Tbet-MAIT cells (Figures S2A and S2B). Further investigation of Rorγt downstream target IL17A, part of the MAIT17 cell signature and known to be produced by MAIT cells even at steady state (Rahimpour et al., 2015), showed that Bcl11b KO TCRβ+MR1t-5-OP-RU+ cells failed to produce IL17A at steady state (Figures 3E and 3F). However, the frequency of IFNγ-producing TCRβ+MR1t-5-OP-RU+ MAIT cells was the same in Bcl11b KO versus WT MAIT cells, in both very low (Figure S3). In mixed BM chimeric mice, although frequency of stage 3 MAIT cells was in large recovered in the absence of Bcl11b (Figures 2C and 2D), frequency of Rorγt+ population and Rorγt MFI remained reduced (Figure 2E). Similarly, the frequency of Rorγt+ cells and Rorγt+ MFI was reduced in the Bcl11b KO TCRβ+MR1t-5-OP-RU+ MAIT cells in the lung of the chimeric mice, as was the frequency of Rorγt+ IL17A+ population (Figures 2H–2K).

These results taken together demonstrate that absence of Bcl11b causes a severe reduction in MAIT cell frequencies and numbers in the thymus and in the lung, with alteration in MAIT17 subset and inability to produce IL17 at steady state, caused by MAIT cell intrinsic defects.

Bcl11b-deficient MAIT cells expand poorly and fail to upregulate IL17A in response to *Salmonella* BRD509 infection, but have elevated granzyme levels

MAIT cells respond to riboflavin metabolites produced by infectious bacteria. We used an established murine infection model with *Salmonella enterica* ser. Typhimurium BRD509 (*Salmonella* BRD509), known to

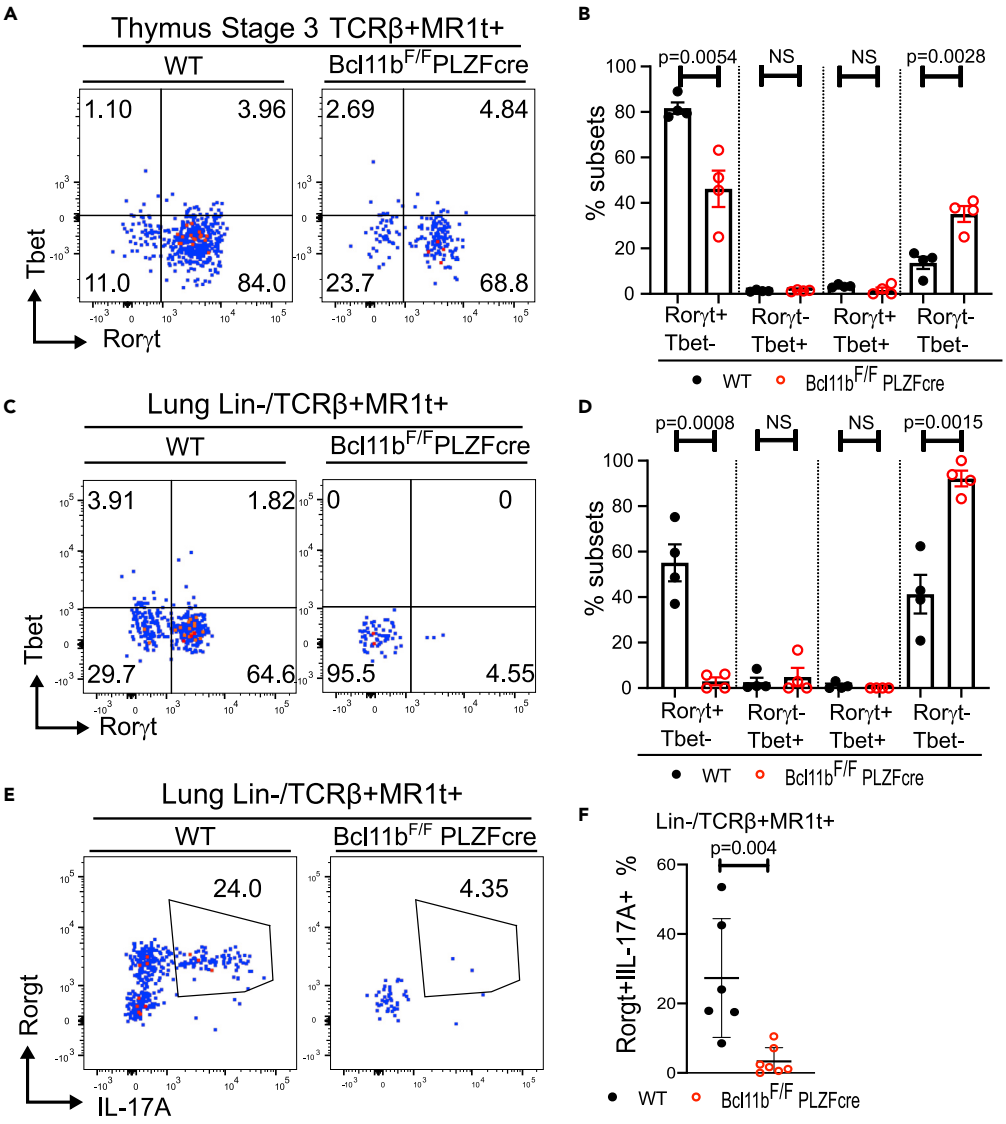

Figure 3. MAIT17 cells are reduced in the absence of Bcl11b in the thymus and periphery and have reduced IL17A production at steady state

(A) Representative dot plots of RORγt and Tbet within stage 3 thymic TCRβ+MR1t-5-OP-RU + cells of Bcl11b$^{F/F}$/PLZFcre and WT mice.

(B) Frequencies of RORγt + Tbet-, RORγt-Tbet+, RORγt + Tbet+, and RORγt-Tbet-within developmental stage 3 TCRβ+MR1t-5-OP-RU + MAIT cells of Bcl11b$^{F/F}$PLZFcre and WT mice. The data are derived from 8 pairs of mice in which two FACS files from the same type of mice (Bcl11b$^{F/F}$/PLZFcre or WT mice) were concatenated.

(C) Representative dot plots of RORγt and Tbet within lin-TCRβ+MR1t-5-OP-RU+ in the lung of Bcl11b$^{F/F}$/PLZFcre and WT mice.

(D) Frequencies of Bcl11b KO and WT RORγt+Tbet-, RORγt-Tbet+, RORγt+Tbet+ and RORγt-Tbet-lin-TCRβ+MR1t-5-OP-RU + MAIT cell subsets in the lung.

(E) Representative dot plots of Bcl11b KO and WT RORγt+ IL17A+ lin-TCRβ+MR1t-5-OP-RU+ MAIT cells in lung.

(F) Frequencies of Bcl11b KO and WT RORγt+ IL17A+ TCRβ+MR1t-5-OP-RU+ MAIT cells in the lung. Each point represents a concatenated file of 2 lung samples run independently.

Data are represented as mean ± SEM. All statistics were conducted as paired t test. $p < 0.05$ was considered significant.

induce a MAIT cell response (Chen et al., 2017). While WT MAIT cells expanded vigorously following infection, Bcl11b-deficient TCRβ+MR1t-5-OP-RU+ MAIT cells remained at much lower frequency and absolute numbers (Figures 4A and 4B). Along this line, frequency of Ki67+ TCRβ+MR1t-5-OP-RU+ MAIT cells was

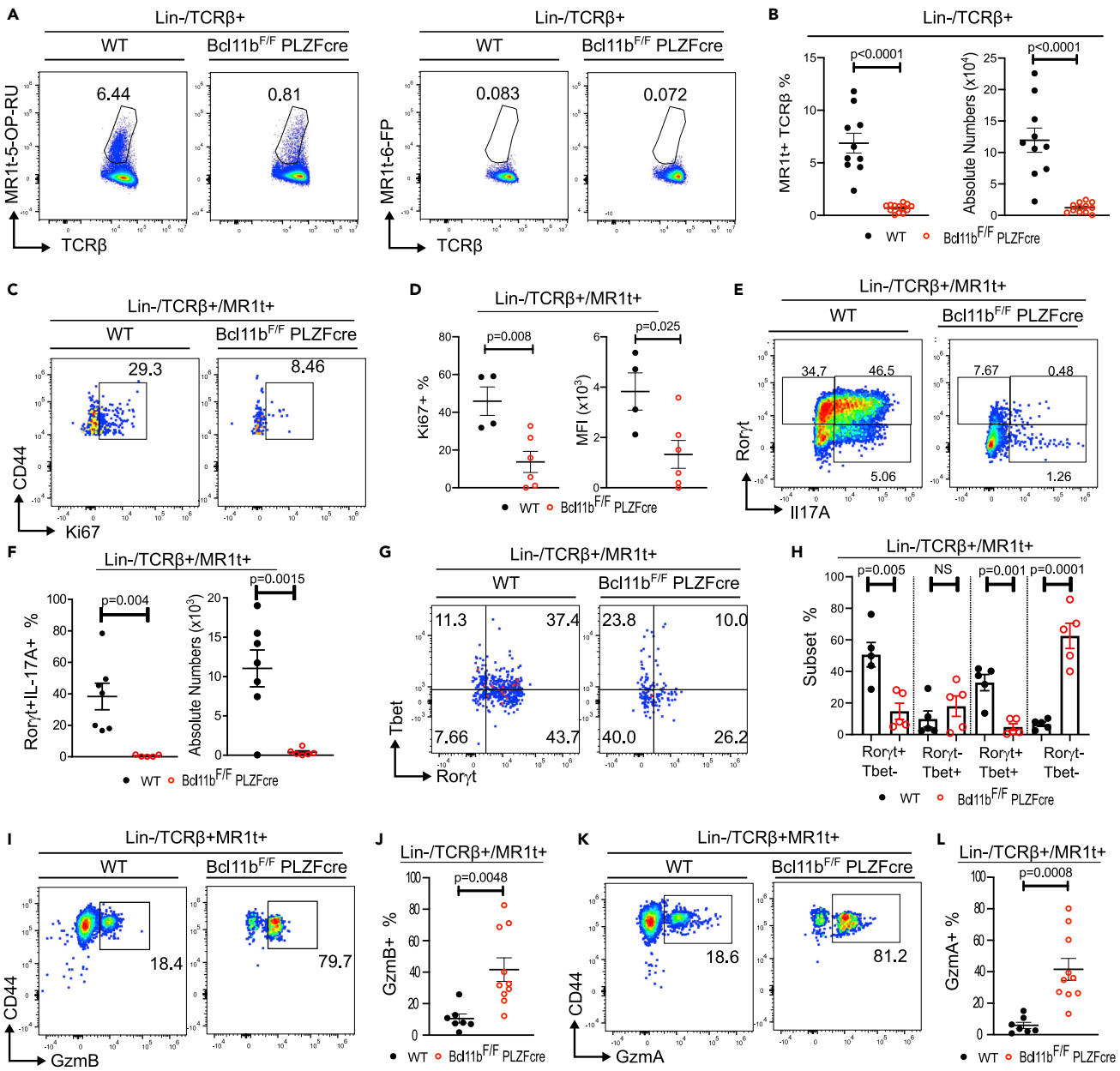

Figure 4. Bcl11b KO MAIT cells fail to expand and produce IL17A during *Salmonella* infection but have elevated granzyme levels

In all experiments Bcl11b$^{F/F}$/PLZFcre and control mice were infected with 10^6 cfu of *Salmonella enterica* ser. Typhimurium BRD509 (*Salmonella* BRD509) intranasally. Mice were euthanized on day 7 post infection.

(A) Representative dot plots of lin- TCRβ+ MR1t-5-OP-RU and control MR1t-6-FP staining in lung of infected Bcl11b$^{F/F}$/PLZFcre and WT mice.

(B) Frequencies and absolute numbers of lin- TCRβ+ MR1t-5-OP-RU+ MAIT cells in lung of infected Bcl11b$^{F/F}$/PLZFcre and WT mice.

(C and D) Representative dot plots (C), frequencies and MFI (D) of Ki67+ CD44+ lung Bcl11b KO and WT lin-TCRβ+MR1t-5-OP-RU+ MAIT cells from infected mice.

(E and F) Representative dot plots (E), frequencies and absolute numbers (F) of Bcl11b KO and WT RORγt+ IL17A+ lin-TCRβ+MR1t-5-OP-RU+ MAIT cells from lung of infected mice.

(G) Representative dot plots of RORγt and Tbet within lin-TCRβ+MR1t-5-OP-RU+ in the lung of Bcl11b$^{F/F}$/PLZFcre and WT infected mice.

(H) Frequencies of Bcl11b KO and WT RORγt+ Tbet-, RORγt-Tbet+, RORγt+Tbet+ and RORγt-Tbet-lin-TCRβ+MR1t-5-OP-RU+ MAIT cell subsets in the lung of Bcl11b$^{F/F}$/PLZFcre and WT infected mice.

(I–L) Representative dot plots (I, K) and frequencies (J, L) of GzmB+ CD44+ (I, J) and GzmA+ CD44+ (K, L) lin-TCRβ+MR1t-5-OP-RU+ MAIT cells in the lung of infected Bcl11b$^{F/F}$/PLZFcre and WT mice.

Data are represented as mean ± SEM. Statistics were conducted as paired t test. $p < 0.05$ was considered significant.

significantly lower in the absence of Bcl11b (Figures 4C and 4D), demonstrating that these cells expand poorly following bacterial infection. However, Bcl11b KO TCRβ+MR1t-5-OP-RU+ MAIT cells did not die more compared to WT following infection (Figure S4A).

It has been established that in response to *Salmonella* BRD509 infection, MAIT cells increase production of IL17A (Chen et al., 2017). While a large proportion of WT TCRβ+MR1t-5-OP-RU+ MAIT cells produced IL17A and upregulated Rorγt following *Salmonella* infection, Bcl11b KO MAIT cells only modestly upregulated RORγt and failed to produce IL17A (Figures 4E and 4F). Similarly, in mixed BM chimeric mice, Bcl11b-deficient TCRβ+MR1t-5-OP-RU+ MAIT cells failed to upregulate Rorγt and produce IL17A following infection (Figures 2L–2O), demonstrating that the defect is intrinsic.

At steady state in the lung, Tbet+ MAIT cells are in very low number. However following bacterial infection, Tbet is known to be upregulated (Wang et al., 2019). Upregulation of Tbet occurred both in WT and Bcl11b KO TCRβ+MR1t-5-OP-RU+ MAIT cells after Salmonella infection (Figures 4G and 4H versus Figures 3C and 3D). However while in WT TCRβ+MR1t-5-OP-RU+ MAIT cells, a large proportion of Tbet+ cells also expressed RORγt, the Tbet+ Bcl11b KO MAIT remained largely negative for Rorγt (Figures 4G and 4H), suggesting that Bcl11b KO MAIT cells upregulate Tbet, but fail to express Rorγt. In fact, the largest proportion of Bcl11b KO MAIT cells was negative for both TFs (Figures 4G and 4H). Bcl11b KO and WT Tbet+ TCRβ+MR1t-5-OP-RU+ MAIT cells produced on average similar levels of IFNγ post infection (Figure S4B).

Granzymes, including GzmA and GzmB, are known to be produced by MAIT cells to kill sensitized targets (Kurioka et al., 2015; Le Bourhis et al., 2010). Both in WT and Bcl11b KO TCRβ+MR1t-5-OP-RU+ MAIT cells, it was the Tbet+ and RORγt-Tbet- MAIT cell subsets which produced granzymes, and not the RORγt + population (Figure S4C). A significantly higher frequency of Bcl11b KO MAIT cells produced GzmA and GzmB compared to WT (Figures 4I–4L), including in mixed chimeras (Figures 2P and 2Q), suggesting an intrinsic defect.

These results taken together demonstrate that Bcl11b is required for MAIT cell expansion during *Salmonella* infection and for supporting MAIT17 cell functional response; however, its absence results in increase in granzyme levels, but not in Tbet or IFNγ.

Bcl11b regulates expression of MAIT17 cell program, CD3 complex and TCR signaling genes at steady state and following *Salmonella* infection

Given the scarce numbers of Bcl11b KO TCRβ+MR1t-5-OP-RU+ MAIT cells in the thymus and the fact that MAIT cells in the periphery resemble thymic stage 3, which are predominantly MAIT17 in NON-Cast C57BL/6 mice (Koay et al. 2016, 2019), we performed RNA-seq on lung Bcl11b KO TCRβ+MR1t-5-OP-RU+ YFP+ (from $Bcl11b^{F/F}$/PLZFcre/R26R-EYFP mice) and WT TCRβ+MR1t-5-OP-RU+ MAIT cells at steady state and following *Salmonella* infection. In our analysis we used as reference for MAIT subsets and developmental stages the results from (Koay et al., 2019), given that this study used MAIT cells from NON-cast C57BL/6 mice, same as our study. As expected, lung WT MAIT cells expressed stage 3 program genes, with a predominant MAIT17 profile (Figures 5A–5D) (Koay et al. 2016, 2019). Lung Bcl11b KO MAIT cells have reduced expression of some of these genes, including *Zbtb16*, *Rorc* and other genes mostly of the MAIT17 program (Figures 5A–5D, Tables S1 and S2).

Some genes belonging to early thymic stages of MAIT cell development, including *Bcl6* were elevated, however others, including *Satb1* and *Tox* (also part of stage 1), were reduced (Figure S5) (Table S5), suggesting a complex role of Bcl11b in regulation of early stage program in mature MAIT cells.

As mentioned above, it was predominantly the MAIT17 cell program genes which were reduced in the absence of Bcl11b while MAIT1 program genes were mostly similarly expressed in Bcl11b KO and WT MAIT cells, and in both at very low levels (Figures 5C and 5D, Tables S3 and S4), supporting the observation that Bcl11b mainly promotes the MAIT17 program at steady state. The differentially expressed genes of MAIT17 cell program included genes for essential TFs (*Rorc*, *c-Maf* and *Zbtb16*). Of note, *Zbtb16* (PLZF) is categorized as belonging to MAIT17 program, given that it is predominantly expressed in in these cells in common mouse laboratory strains (Koay et al., 2019). Essential MAIT17 genes, including those for *Il17a*, *Il23r*, *CCR6*, cytokines and their receptors (*Il7ra*, *Il18r1*, *Il1r1*, *Il17rb*, *Il17re*, *Il27ra*), chemokine receptors

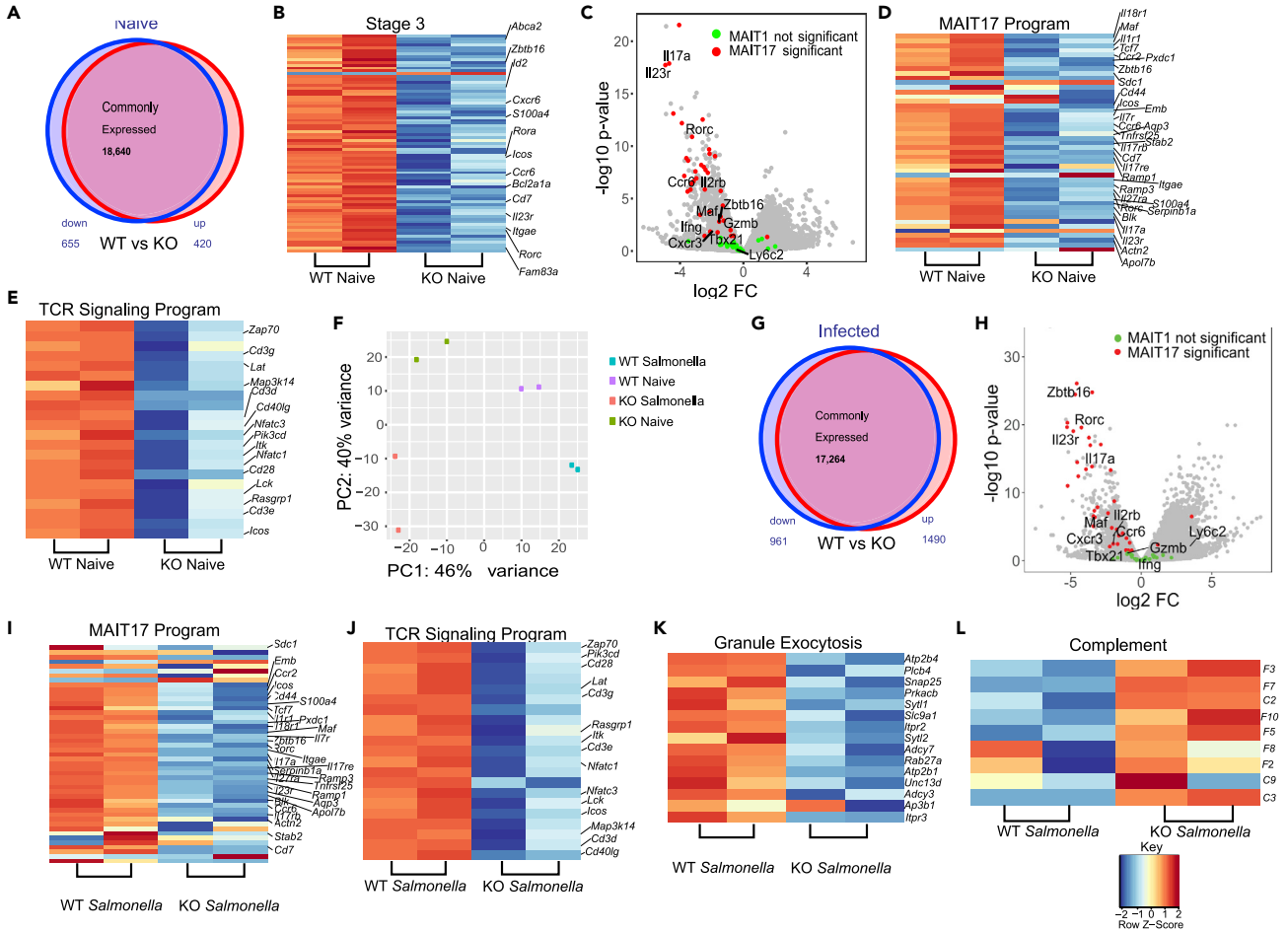

Figure 5. Bcl11b sustains MAIT17, TCR signaling and cytotoxic granule exocytosis programs but represses complement genes in MAIT cells

All RNA-seq experiments were performed on sorted lin-TCRβ+MR1t-5-OP-RU+ MAIT cells from lung of Bcl11b$^{F/F}$/PLZFcre/R26R-EYFP mice and WT control mice at steady state (A-F) or infected with *Salmonella* Typhimurium BRD509 (*Salmonella*) intranasally, day 7 post-infection (F-L). For Bcl11b$^{F/F}$/PLZFcre/R26R-EYFP mice, in addition to lin-TCRβ+ MR1t-5-OP-RU+, sorting was conducted on YFP+ cells.

(A) Venn diagram depicting differentially expressed genes (significantly downregulated in blue and significantly upregulated in red) in Bcl11b KO and WT MAIT cells from uninfected mice.

(B) Heatmaps of differentially expressed stage 3 genes.

(C) Volcano plot of MAIT1 and MAIT17 genes in Bcl11b KO versus WT MAIT cells from mice at steady state.

(D) Heatmap of differentially expressed MAIT17 program.

(E) Heatmap of differentially expressed TCR signaling program genes in Bcl11b KO and WT MAIT cells from lung of uninfected mice. (n = 2).

(F) Principal component analysis (PCA) of MAIT cell RNA-seq from lung of Bcl11b$^{F/F}$/PLZFcre/R26R-EYFP and WT mice at steady state or infected with *Salmonella*. (n = 2).

(G) Venn diagram depicting differentially expressed genes (significantly downregulated in blue and significantly upregulated in red) from Bcl11b KO and WT MAIT cells from *Salmonella*-infected mice.

(H) Volcano plot of MAIT17 and MAIT1 cells in Bcl11b KO versus WT MAIT cells from lung of mice infected with *Salmonella*.

(I–L) Heatmaps of MAIT17 program (I), TCR signaling (J), cytotoxic granule exocytosis (K) and complement (L) genes differentially expressed in Bcl11b KO and WT MAIT cells from *Salmonella*-infected mice. (n = 2). False discovery rate (FDR)–adjusted p values were calculated using the Benjamini-Hochberg method, with a significance cutoff of adjusted $p < 0.05$.

(*Ccr2*), specific markers, receptors and signaling molecules (*Cd44*, *Icos*, *Itgae*, *Sdc1* (CD138), *Blk*, *Pxdc1*, *Emb*, *Tnfrsf25*, *Aqp3*, *Stab2*, *Cd7*, *Ramp1*, *Ramp3*, *S100a4*, *Actn2* and *Apol7b*) (Koay et al., 2019) have reduced expression in lung Bcl11b KO MAIT cells at steady state (Figures 5C and 5D, and Table S3). From the few genes classified as belonging to the MAIT1 program downregulated in Bcl11b KO MAIT cells were *Klrk1*, *Fgl2*, *Il2rb* and *Cd28* (Table S4), however mRNA levels for *Tbx21*, *Ifnγ* and *Tnf* remained similar between Bcl11b KO and WT MAIT cells at steady state (Figure S6).

In addition, RNA-seq analysis showed that Bcl11b KO MAIT cells have reduced mRNA levels encoding numerous genes belonging to TCR signaling, including for: *CD3* complex, *Cd28, Icos, Pdcd1, Lck, Itk, Zap70, Rasgrp1, Grap2, Card11, Lat, Map3k14, Nfatc1, Nfatc3, Nfkbie, Pik3cd, Pik3cg, Pdcd1, Ptprc,* and *Cd40l* (Figures 5E and Table S6), demonstrating a critical role for Bcl11b in sustaining TCR signaling program.

We further conducted RNA-seq analysis of Bcl11b KO TCRβ+MR1t-5-OP-RU+ YFP+ (from Bcl11b$^{F/F}$/PLZFcre/R26R-EYFP mice) and WT TCRβ+MR1t-5-OP-RU+ MAIT cells following infection with *Salmonella* BRD509. Principal component analysis (PCA) clearly separated WT MAIT cells from infected and uninfected mice, Bcl11b KO MAIT cells of uninfected mice and infected mice, and additionally the Bcl11b KO versus WT MAIT cells from both uninfected and infected mice (Figure 5F). Analysis of differentially expressed genes between Bcl11b KO and WT TCRβ+MR1t-5-OP-RU+ MAIT cells from Salmonella-infected mice shows that MAIT17 cell program genes further remained reduced in the Bcl11b KO MAIT cells compared to WT MAIT cells from infected mice, while MAIT1 genes were similarly expressed for the most, with a trend in *Tbx21* downregulation (Figures 5G–5I and S6, Tables S3 and S6). Reduced MAIT17 mRNAs included those for the TF *Rorc, Zbtb16, c-MAF,* essential MAIT17 cytokines and receptors *Il17a*, *IL17f, Il23r*, *CCR6*, cytokines and receptors (*Il7ra*, *Il18r1*, *Il1r1*, *Il17rb, Il17re, Il27ra*), chemokine receptors (*Ccr2*), specific markers, other receptors and signaling molecules (*Cd44*, *Icos*, *Blk*, *Itgae*, *Pxdc1, Emb, Tnfrsf25, Ramp1, Ramp3, S100a4, Serpinb1a, Actn2,* and *Apol7b*) (Figures 5H and 5I, Table S3). Expression of TCR signaling genes also remained significantly diminished in Bcl11b KO MAIT cells following *Salmonella* infection, including mRNAs for CD3 complex, *Cd28, Icos, Pdcd1, Lck, Zap70, Lat, Itk, Rasgrp1, Grap2, Card11, CD40l, Map3k14, Nfatc1, Nfatc2* and *Nfatc3* (Figures 5J and Table S6).

Given the increased levels of GzmA and GzmB in Bcl11b KO cells MAIT cells from infected mice, we further evaluated granzyme mRNAs and found their levels not differentially expressed between Bcl11b KO and WT MAIT cells (Figure S7). These results suggest that the accumulation of GzmA and GzmB in the KO MAIT cells may occur through a distinct mechanism than regulation of their expression. In line with this, multiple genes belonging to cytotoxic CGE pathway, including *Atp2b4, Plcb4, Snap25, Prkacb*, *Sytl1, Slc9a1, Itpr2, Sytl2, Adcy7, Rab27a*, *Atp2b1*, *Unc13d*, *Adcy3,* and *Itpr3* (Haddad et al., 2001; Kurioka et al., 2015; Kwong et al., 2000; Ménasché et al., 2008; Stinchcombe et al., 2001; Holt et al., 2008), were downregulated in the absence of Bcl11b (Figure 5K), suggesting that accumulation of granzymes in the absence of Bcl11b in TCRβ+MR1t-5-OP-RU+ MAIT cells may be caused by this reduction.

Among genes upregulated in the absence of Bcl11b were those belonging to the complement pathway, but not to NK or myeloid genes (Figure 5L and data not shown), known to be derepressed in other mature T cells in the absence of Bcl11b (Drashansky et al., 2019). Complement genes are derepressed in the absence of Bcl11b in other T cells as well (Helm and Avram, unpublished).

These results demonstrate that Bcl11b sustains MAIT17 and TCR signaling programs at steady state and following *Salmonella* infection. Additionally, Bcl11b is required to support expression of CGE program genes with role in granzyme release, and restrains complement gene expression in lung MAIT cells following infection.

BCL11B binds at genomic regions with enriched H3K27ac of the MAIT17 and MAIT1 programs and at core TCR signaling genes in human MAIT cells

BCL11B is highly conserved between humans and mice (Avram et al. 2000, 2002; Avram and Califano 2014). Our previous results showed that BCL11B bound at many common genes in human and mouse Treg cells, and moreover the binding regions were situated at similar locations within the homologous gene (Drashansky et al., 2019). Given these similarities and the fact that MAIT cells are in reduced numbers in mice, we performed BCL11B ChIP-seq and H3K27Ac ChIP-seq on human peripheral blood CD3+CD161+TCRVα7.2+ MAIT cells, to identify the genes bound by BCL11B and the associated regulomes. Peak annotation showed BCL11B binding at intergenic regions, introns and promoters in human MAIT cells (Figure 6A). Just as we previously reported in CD4$^+$ T cells and Treg cells (Lorentsen et al., 2018; Drashansky et al., 2019), the top binding motif for BCL11B was ETS, with a preference for Fli1, the second was RUNX, while AP-1 was the third (Figure 6B). Analysis of BCL11B-binding motifs correlated with H3K27Ac peaks revealed two ETS motifs as top (Elk4, the first, and Fli1 reverse, the second), while RUNX was the third (Figure 6C), suggesting that BCL11B uses ETS and RUNX motifs to control putative enhancer activity in MAIT cells.

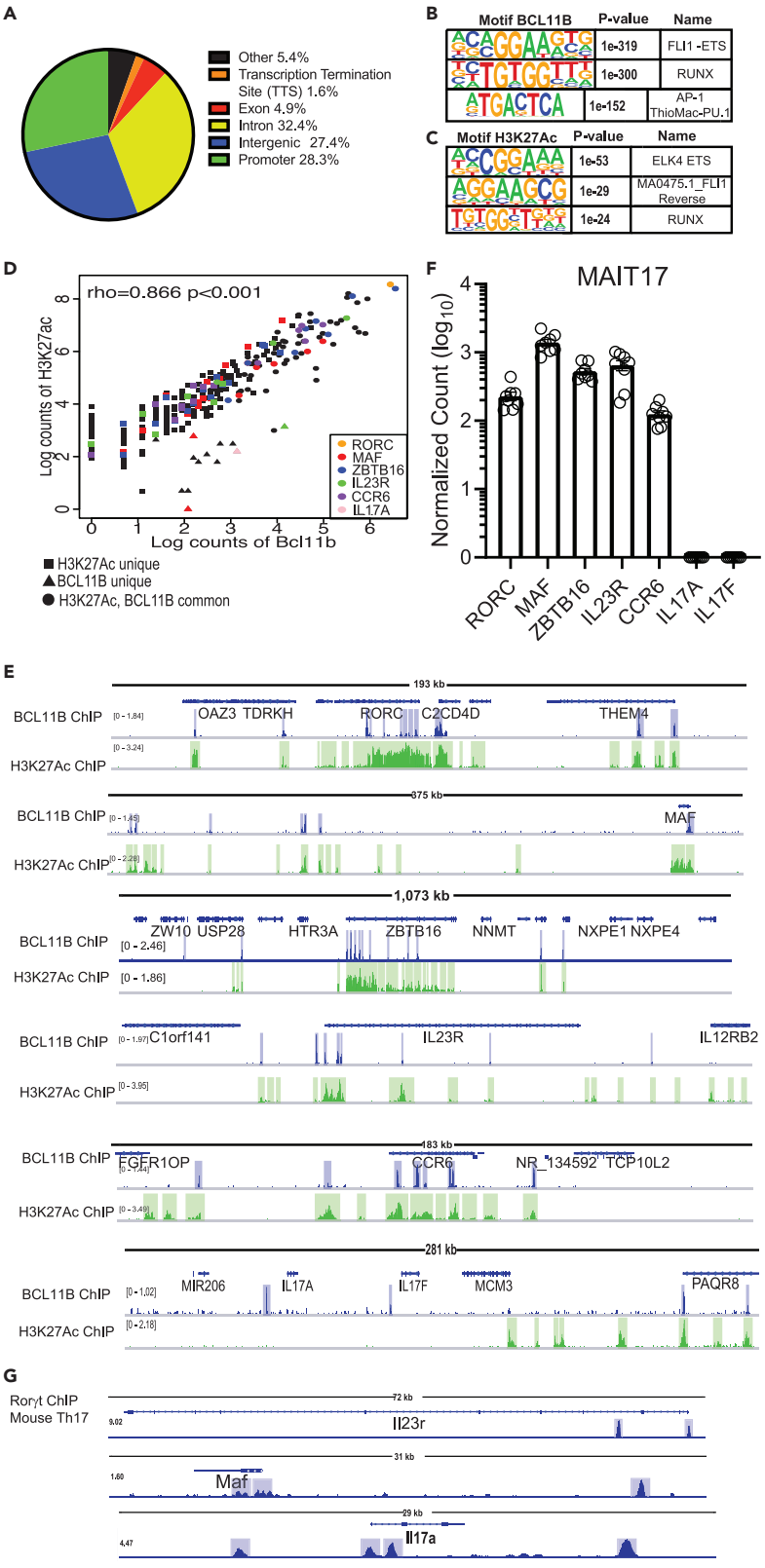
A
Other 5.4%
Transcription Termination Site (TTS) 1.6%
Exon 4.9%
Intron 32.4%
Intergenic 27.4%
Promoter 28.3%
B
Motif BCL11B
P-value
Name
1e-319
FLI1 -ETS
1e-300
RUNX
1e-152
AP-1 ThioMac-PU.1
C
Motif H3K27Ac
P-value
Name
1e-53
ELK4 ETS
1e-29
MA0475.1_FLI1 Reverse
1e-24
RUNX
D
rho=0.866 p<0.001
Log counts of H3K27ac
Log counts of Bcl11b
RORC
MAF
ZBTB16
IL23R
CCR6
IL17A
H3K27Ac unique
BCL11B unique
H3K27Ac, BCL11B common
F
MAIT17
Normalized Count (log10)
RORC
MAF
ZBTB16
IL23R
CCR6
IL17A
IL17F
E
BCL11B ChIP
H3K27Ac ChIP
OAZ3 TDRKH
RORC C2CD4D
THEM4
MAF
ZW10 USP28
HTR3A
ZBTB16
NNMT
NXPE1 NXPE4
C1orf141
IL23R
IL12RB2
FGFR1OP
CCR6
NR_134592 TCP10L2
MIR206
IL17A
IL17F
MCM3
PAQR8
G
Rorγt ChIP
Mouse Th17
Il23r
Maf
Il17a

Figure 6. BCL11B binds at H3K27Ac-rich regions of key genes of MAIT17 program in human MAIT cells from healthy donors

(A) Peak distribution of BCL11B binding sites genome-wide in human MAIT cells sorted as CD3+CD161+TCRVα7.2+ from PBMCs of healthy donors. (B) Top 3 BCL11B binding motifs in human MAIT cells.

(C) Top 3 BCL11B motifs overlapping with H3K27Ac peaks. CD3+CD161+TCRVα7.2+ were sorted from PBMCs derived from nine donors (BCL11B ChIP-seq) and two donors (H3K27Ac ChIP-seq).

(D) Spearman's Correlation plot of BCL11B binding intensity with H3K27Ac peaks at MAIT17 signature genes. Several genes of the MAIT17 program are listed.

(E) Integrative Genomics Viewer (IGV) visualization at *RORC, MAF, ZBTB16, IL23R, CCR6* and *IL17A* and *IL17F* loci of BCL11B ChIP-seq (track 1) and H3K27Ac ChIP-seq (track 2) in human MAIT cells sorted from PBMCs of healthy donors.

(F) Normalized counts in $\log_{10}$ format for *RORC, MAF, ZBTB16, IL17A, IL17F, IL23R, CCR6* in blood MAIT cells of healthy donors. Data analyzed from (Dias et al., 2018). n = 8. Data are represented as mean ± SEM.

(G) IGV visualizations of Rorγt ChIP-seq in murine Th17 cells at *IL23r, Maf*, and *IL17a* loci. Data analyzed from (Ciofani et al., 2012). Blue and green highlights indicate significant ChIP-seq peaks. ChIP-seq scale bar normalized to sequences per million reads.

We focused on genomic regions associated with essential programs of MAIT cells. Analysis using Spearman's Correlation Algorithm showed high correlation of BCL11B binding and H3K27Ac at human MAIT17 signature genes (Figure 6D). *RORC* and *ZBTB16* showed the highest correlation, followed by *CCR6, IL23R,* and *c-MAF* (Figure 6D). These MAIT17 program genes had decreased expression in mouse Bcl11b-deficient MAIT cells both at steady state and in infection (Figures 5C, 5D, 5H, and 5I). *RORC, ZBTB16,* c-*MAF, IL23R,* and *CCR6* were all expressed in MAIT cells from healthy donors (Figure 6F, compiled from (Dias et al., 2018)). While BCL11B bound upstream of *IL17A* and *IL17F* genes, H3K27ac was very low at these loci, including in regions where BCL11B bound (Figure 6E), and neither *IL17A* or *IL17F* genes were expressed in the blood MAIT cells of healthy donors (Figure 6F, compiled from (Dias et al., 2018)). Thus, *IL17* genes are not expressed in human MAIT cells from healthy volunteers, and though BCL11B binds at these genes, additional factors are needed for expression of these genes in human MAIT cells.

While no data is available on Rorγt ChIP-seq in MAIT cells, the analysis of Rorγt ChIP-seq in murine Th17 cells (Ciofani et al., 2012) showed that Rorγt bound at homologs genes to those bound by BCL11B in human MAIT17 cells, including at *c-MAF, IL23R* and *IL17A* (Figure 6G), suggesting that BCL11B and Rorγt may cooperate in regulating gene expression of key type 3 (17) program genes.

Surprisingly, Spearman's Correlation analysis showed significant correlation of BCL11B binding and H3K27Ac at human MAIT1 signature genes (Figure 7A), despite that in the absence of BCL11B, these genes were not significantly changed in expression in murine MAIT cells (Figures 5C and 5H). Binding was observed at *TBX21, CXCR3, GZMA, GZMB, GZMK, SLAMF7* and *IFNγ*, correlated with enriched H3K27Ac (Figure 7B). All MAIT1 program genes are expressed in human MAIT cells from healthy donors (Figure 7C) (compiled from (Dias et al., 2018)). These results thus suggest that in human MAIT cells, in addition to control MAIT17 program, BCL11B may be implicated in the control of essential genes of the MAIT1 program, dissimilar to mouse.

Genes encoding the CD3 complex and TCR signaling were downregulated in the absence of BCL11B in murine MAIT cells at steady state and in infection (Figures 5E and 5J). In human MAIT cells we found a strong correlation between BCL11B binding and H3K27Ac peaks at CD3 complex and TCR signaling program genes (Figure 8A). Among the bound genes which showed strong correlations, were CD3 complex genes, *CD28, ICOS, ITK, LCK,* and *PIK3CD* (Figure 8B). These genes are all expressed in MAIT cells isolated from peripheral blood of healthy donors (Figure 8C) (compiled from (Dias et al., 2018)).

In addition to genes implicated in MAIT17, MAIT1 and TCR signaling programs, BCL11B showed significant binding at intron 3 of its own locus, as well as at a region located approximately 200kb from its 3′ end in a gene empty island, as well as at a location in close vicinity of the +845kb enhancer, also conserved in Treg cells (data not shown). While binding at the 3′ downstream locations showed minimal H3K27Ac, binding at the intron overlapped with high H3K27Ac (Figure 8D), suggesting that BCL11B may play a role in sustaining its own expression in these cells.

In addition, BCL11B bound at flanking regions of *C2* and *C3* complement genes, depressed in the absence of BCL11B in murine MAIT cells, in areas with H3K27Ac peaks, despite that overall H3K27Ac was almost absent at *C2* and *C3* complement genes (Figure S8), suggesting a putative role of BCL11B in repressing these innate genes in MAIT cells.

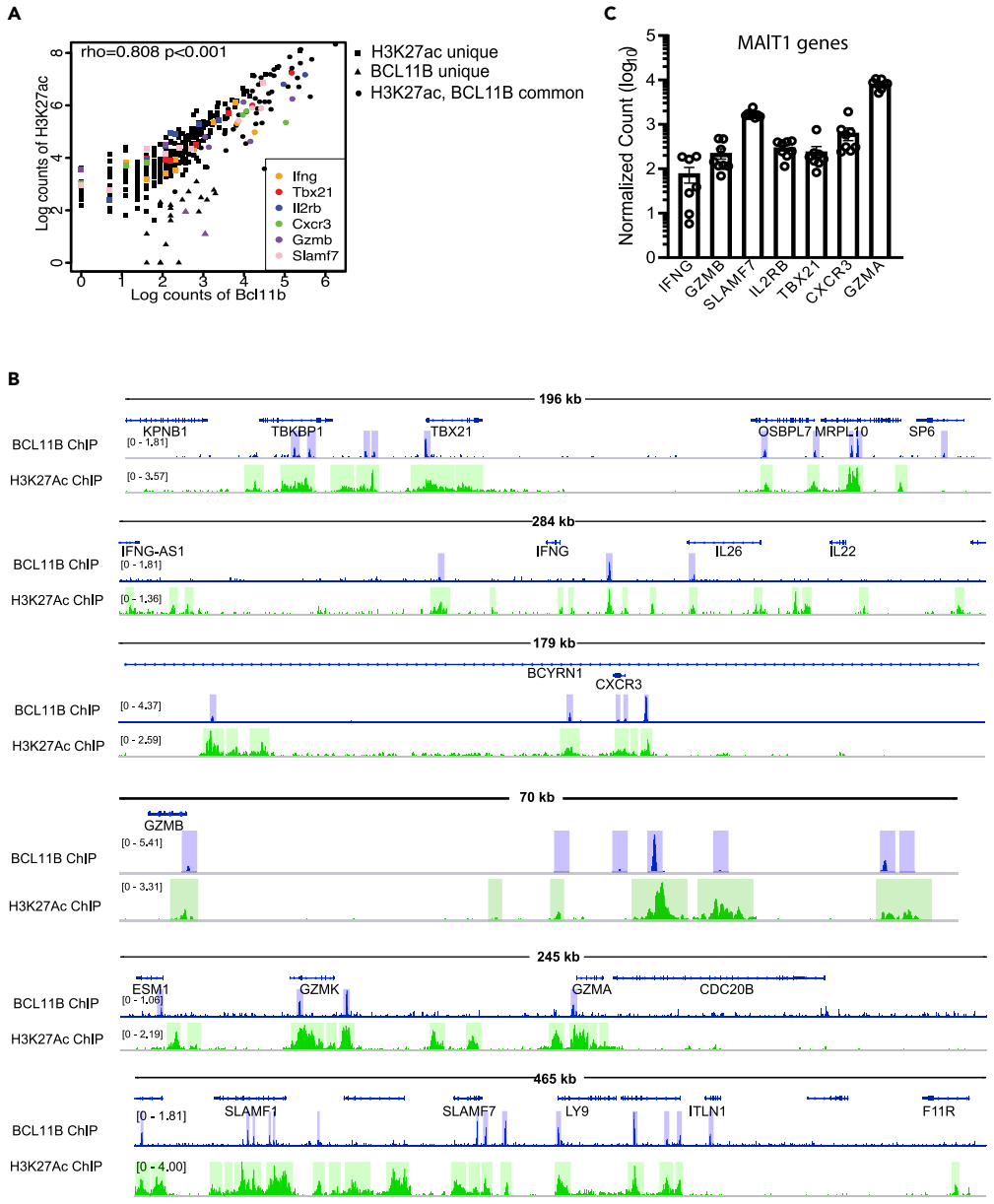

Figure 7. BCL11B binds at H3K27Ac-rich regions of key genes of MAIT1 program in human MAIT cells from healthy donors

(A) Spearman's Correlation plot of BCL11B binding intensity with H3K27Ac peaks at MAIT1 signature genes. Several genes of the MAIT1 program are listed.

(B) Integrative Genomics Viewer (IGV) visualization at *TBX21*, *IFNγ*, *CXCR3*, *SLAMF7*, *GZMB*, *GZMA*, and *GZMK* loci of BCL11B ChIP-seq (track 1) and H3K27Ac ChIP-seq (track 2) in human MAIT cells sorted from PBMCs of healthy donors. CD3+CD161+TCRVα7.2+ were sorted from PBMCs derived from nine donors (BCL11B ChIP-seq) and two donors (H3K27Ac ChIP-seq).

(C) Normalized counts in $\log_{10}$ format for *TBX21*, *IFNγ*, *CXCR3, GZMB, GZMA, and SLMF7* in blood MAIT cells of healthy donors. Data analyzed from (Dias et al., 2018). n = 8. Data are represented as mean ± SEM. Blue and green highlights indicate significant ChIP-seq peaks. ChIP-seq scale bar normalized to sequences per million reads.

These results taken together show that BCL11B binds in human MAIT cells at genes homologous to the mouse genes that have the expression dysregulated in its absence, including at essential MAIT17, CD3 complex and TCR signaling programs, as well as at some complement genes. Many of the bound regions are associated with increased H3K27Ac, suggesting a critical role of BCL11B in the control of regulomes

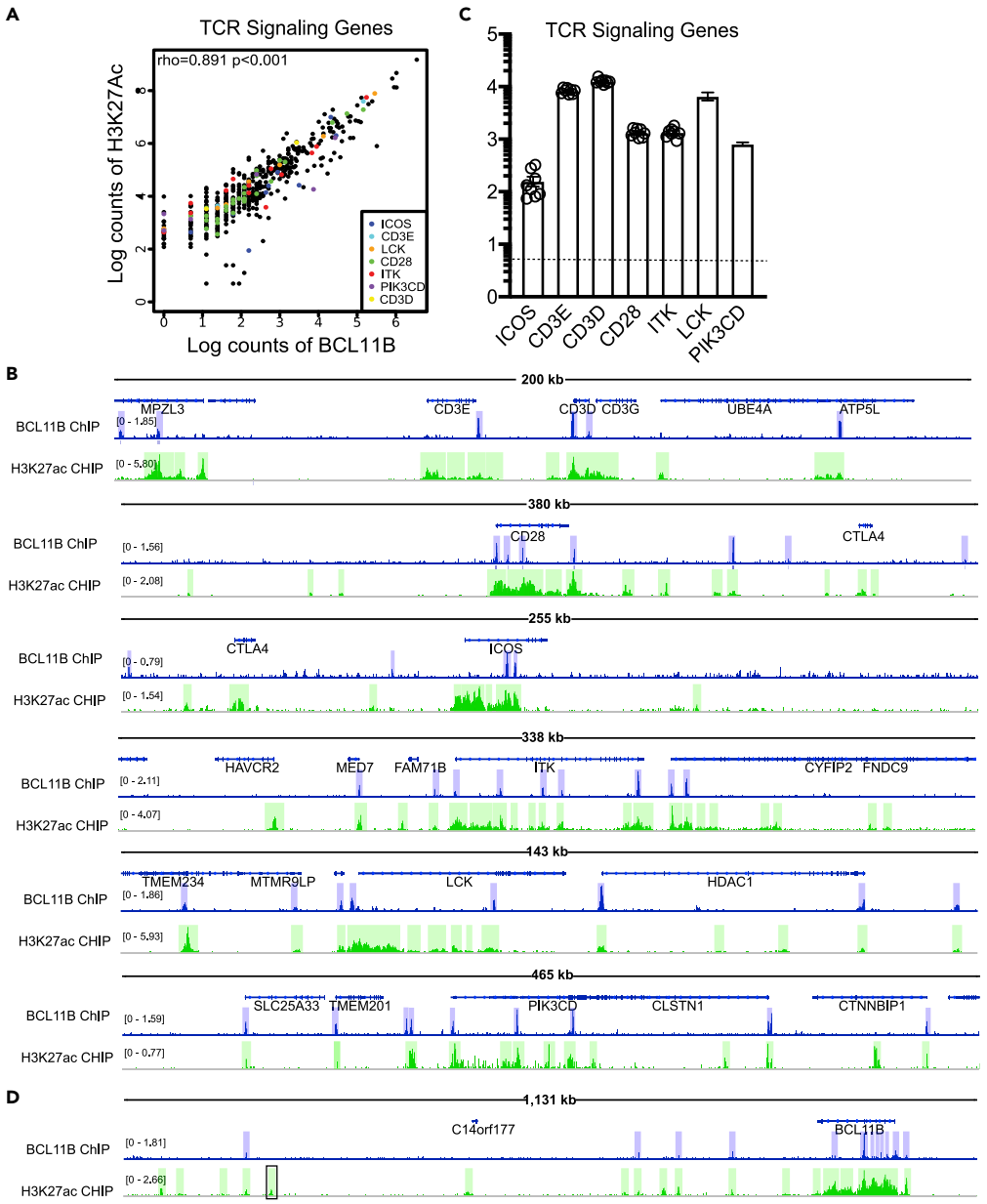

Figure 8. BCL11B binds at essential genes of TCR signaling program and at BCL11B locus in human MAIT cells from healthy donors at regions with high H3K27Ac

(A) Spearman's Correlation plot of BCL11B binding intensity with H3K27Ac peaks at TCR Signaling genes. Several genes of the TCR program are listed.

(B) Integrative Genomics Viewer (IGV) visualization at TCR signaling loci: CD3 complex, *CD28*, *ICOS*, *ITK*, *LCK*, and *PIK3CD* of BCL11B ChIP-seq (track 1) and H3K27Ac ChIP-seq (track 2) in human MAIT cells sorted from PBMCs of healthy donors.

(C) Normalized counts in $\log_{10}$ format for TCR signaling mRNAs from blood MAIT cells of healthy donors. Data analyzed from (Dias et al., 2018). n = 8.

(D) IGV at BCL11B locus of BCL11B ChIP-seq (track 1) and H3K27Ac ChIP-seq (track 2) in human MAIT cells. In B and D, blue and green highlights indicate significant ChIP-seq peaks. In D, the position of +845kb enhancer is indicated in black rectangular. ChIP-seq scale bar normalized to sequences per million reads.

with roles in these programs. Although in mouse MAIT cells Bcl11b did not appear to regulate MAIT1 program, BCL11B did bind at essential MAIT1 genes in human MAIT cells in regions associated with putative active enhancers, suggesting a different role of BCL11B in the control of MAIT1 program in humans and mice.

DISCUSSION

The TFs PLZF and RORγt have been demonstrated to be essential in MAIT cells (Okada et al., 2015; Koay et al. 2016, 2019; Godfrey et al., 2019). In this study, we established that BCL11B has a fundamental role in MAIT cells and positioned BCL11B upstream of PLZF and RORγt. Absence of Bcl11b in mice affected MAIT cell numbers and impacted particularly MAIT17 program. MAIT17 cells were not only reduced in the thymus and lung in the absence of Bcl11b, but they completely fail to produce IL17A even in conditions of bacterial infection. Transcriptomics analysis shows that Bcl11b controls the MAIT17 cell program both at steady state and in infection conditions. In addition, in human MAIT cells BCL11B did not only bind at *RORC* locus, but also at essential genes of the MAIT17 cell program, including at *ZBTB16*, *MAF*, *IL23R, CCR6,* and *IL17A*. Importantly binding at MAIT17 program genes was in locations enriched in H3K27Ac, some of which possibly novel enhancers. It will be important to compare the binding and H3K27Ac activity at these genes in MAIT cells versus iNKT cells, given the opposite role of BCL11B in these two lineages, namely sustaining the expression of MAIT17 program genes in MAIT cells, but blocking the expression of iNKT17 program in iNKT cells (Uddin et al., 2016). Conversely, it possible that BCL11B binds in a similar manner at *ZBTB16* locus both in MAIT cells and iNKT cells, given that BCL11B positively controlled the expression of this gene both in iNKT cells (Uddin et al., 2016) and MAIT cells (this study). This is different from DN2 thymocytes, where Bcl11b represses *Zbtb16* expression, likely associated with the repression of the innate-like programs in these cells (Hosokawa et al. 2018, 2020). Thus, Bcl11b plays divergent roles in regulation of *Zbtb16* gene expression in DN2 thymocytes versus MAIT cells and iNKT cells, repressing its expression in DN2 thymocytes, but positively controlling its expression in the innate-like T cells, MAIT and iNKT. Binding of BCL11B in human MAIT cells at *ZBTB16* locus seems to occur at similar location to its binding in murine DN3 cells (Hosokawa et al., 2020), despite the different outcomes of its ablation in the two cell types. It will be of interest to establish what switches BCL11B from suppressing *ZBTB16* expressing in DN2 thymocytes to promoting its expression in the innate-like cells T cells such as iNKT and MAIT cells, and determine how BCL11B regulates specific enhancer activity and chromatin accessibility.

Further comparisons are important as well, given that in Th2 cells, *Rorc* and Th17 program was derepressed in the absence of Bcl11b (Lorentsen et al., 2018), again supporting the idea of a complex subset/lineage specific behavior of Bcl11b in regulation of these programs and TFs, rather than a common generalized role. This is surprising, given that in MAIT cells, CD4+ T cells and Treg cells, the top two binding motifs for Bcl11b are ETS and RUNX (Lorentsen et al., 2018; Drashansky et al., 2019). In ILC2s, similarly to Th2 cells and iNKT cells, *Rorc* and type 3 program were derepressed (Califano et al., 2015), however top Bcl11b binding motifs seem to be divergent in these cells (Hosokawa et al., 2020). Molecular details on how Bcl11b restricts *Rorc* expression and type 3 program in primary ILC2s, Th2 effector cells and iNKT cells, but supports its expression in MAIT cells, are under investigation.

Binding of BCL11B at MAIT17 program genes was specific for MAIT cells and did not occur in the divergent Treg cells, in which instead BCL11B bound at Treg specific genes ((Drashansky et al., 2019) and data not shown), further supporting the notion that in divergent T cells, BCL11B specifically controls cell specific programs in addition to T cell-broad programs, such as TCR signaling. Indeed, BCL11B also plays a generalized common role in T cells, including in MAIT cells, in controlling TCR signaling program. BCL11B bound at the *CD3* complex, *CD28*, *ICOS*, *ITK*, *LCK,* and *PIK3CD* loci. Binding at these locations in MAIT cells was associated with H3K27Ac peaks, indicative of putative active enhancers. Along this line, TCR signaling program genes were reduced in murine Bcl11b KO MAIT cells both at steady state and in infection. Thus, BCL11B not only initiates expression of these genes at commitment stage, but further it is needed to sustain their expression.

BCL11B bound in human MAIT cells at MAIT1 program genes, including at *TBX21*, *IFNγ*, *GZMB* and *GZMA*, at regions associated with putative active enhancers, even though these genes were not differentially expressed in mouse MAIT cells at steady state or during infection. One possibility may stand in the more pronounced MAIT1 nature of human MAIT cells as compared to the mouse MAIT cells, also reflected in the scarcity of MAIT1 cells in mice, or differences in BCL11B-mediated regulation in the two species. Though

mRNAs for *Gzmb* and *Gzma* were not different in mouse BCL11B-deficient MAIT cells, protein levels were elevated. Related to this, numerous genes belonging to cytotoxic granule exocytosis pathway, were down-regulated, suggesting that increased granzyme levels in Bcl11b-deficient MAIT cells are likely due to their accumulation related to the reduction in this pathway. However in human MAIT cells BCL11B bound at *GZMB* and *GZMA* loci, as well as at genes of the CGE pathway, suggesting a complex role for BCL11B in regulation of pathways involved in Granzyme expression and production in human MAIT cells.

In summary, our findings demonstrate that BCL11B is an essential MAIT cell TF and regulates fundamental programs of these cells, including MAIT17 and TCR signaling programs, and potentially MAIT1 program in human MAIT cells. In addition, our study positions BCL11B in the network of TFs that regulate MAIT cells, specifically upstream of PLZF and RORγt. Importantly, BCL11B does not only control MAIT17 program through RORγt, but also directly, by binding to genes of this pathway including at c-*MAF*, *IL17A*, *CCR6* and *IL23R*. Understanding how programs and responses of these cells are regulated will help in designing future therapies for bacterial infections and anti-tumor immune responses.

Limitations of the study

One limitation is the reduced number of MAIT cells in common laboratory mice and thus the impossibility to conduct Bcl11b ChIP-seq in murine MAIT cells, which would have provided a more clear picture on the programs commonly and differentially regulated by BCL11B in humans versus mice.

Resource availability

Lead contact

Further information and requests for resources should be directed to the lead contact, Dr. Dorina Avram, Dorina.avram@moffitt.org.

Material availability

No new or unique reagents were generated by this study.

Data and code availability

RNA-seq and ChIP-seq data shown in this study have been deposited in the Gene Expression Omnibus database with accession GEO: GSE145779. All data needed to evaluate the conclusions in the paper are present in the paper and/or the supplemental information. Additional data and code related to this paper may be requested from the authors.

METHODS

All methods can be found in the accompanying transparent methods supplemental file.

SUPPLEMENTAL INFORMATION

Supplemental information can be found online at https://doi.org/10.1016/j.isci.2021.102307.

ACKNOWLEDGMENTS

We thank Dr. Stephen J. McSorley of UC- Davis for *Salmonella enterica* ser. Typhimurium BRD509. We gratefully acknowledge the National Institutes of Health Tetramer Core Facility (NIH TCF) for providing the MR1 monomers. We gratefully acknowledge C. Tao and P. Kumar for technical assistance and Xiaoping Luo for maintaining the mouse colony. Funding: This work was supported by NIH grants R01AI067846, R01AI33623 (to D.A.) and UF Health Cancer Center (to D.A.), R01AI33623 (to B.K.), R01DK105562 and R01AI132391 (to L.Z.) and 2T32DK074367 (to T.T.D.).

AUTHOR CONTRIBUTIONS

Conceptualization: T.T.D., E.H., and D.A. Experimental design: T.T.D., E.H. L.M., Z.H., and D.A. Methodology: T.T.D., N.C., E.H., J.C., and D.A. Performed experiments: T.T.D., N.C., E.H., P.C., X.C., and J.C. Software: T.T.D., E.H., L.M., X.H. Formal analysis: T.T.D., N.C., E.H., J.C. L.M., Z.H., and D.A. Resources: D.A., B.K, L.Z., and W.Z. Data curation: T.T.D. and D.A. Writing and editing: T.T.D., E.H., N.G., and D.A.

DECLARATION OF INTERESTS

The authors declare no competing interests.

INCLUSION AND DIVERSITY

We worked to ensure sex balance in the selection of non-human subjects.

Received: July 1, 2020
Revised: November 2, 2020
Accepted: March 10, 2021
Published: April 23, 2021

REFERENCES

Abboud, G., Stanfield, J., Tahiliani, V., Desai, P., Hutchinson, T.E., Lorentsen, K.J., Cho, J.J., Avram, D., and Salek-Ardakani, S. (2016). Transcription factor Bcl11b controls effector and memory CD8 T cell fate decision and function during poxvirus infection. Front. Immunol. *7*, 425.

Albu, D.I., Feng, D., Bhattacharya, D., Jenkins, N.A., Copeland, N.G., Liu, P., and Avram, D. (2007). BCL11B is required for positive selection and survival of double-positive thymocytes. J. Exp. Med. *204*, 3003–3015.

Albu, D.I., Vanvalkenburgh, J., Morin, N., Califano, D., Jenkins, N.A., Copeland, N.G., Liu, P., and Avram, D. (2011). Transcription factor Bcl11b controls selection of invariant natural killer T-cells by regulating glycolipid presentation in double-positive thymocytes. Proc. Natl. Acad. Sci. U S A *108*, 6211–6216.

Avram, D., and Califano, D. (2014). The multifaceted roles of Bcl11b in thymic and peripheral T cells: impact on immune diseases. J. Immunol. *193*, 2059–2065.

Avram, D., Fields, A., Pretty on Top, K., Nevrivy, D.J., Ishmael, J.E., and Leid, M. (2000). Isolation of a novel family of C(2)H(2) zinc finger proteins implicated in transcriptional repression mediated by chicken ovalbumin upstream promoter transcription factor (COUP-TF) orphan nuclear receptors. J. Biol. Chem. *275*, 10315–10322.

Avram, D., Fields, A., Senawong, T., Topark-Ngarm, A., and Leid, M. (2002). COUP-TF (chicken ovalbumin upstream promoter transcription factor)-interacting protein 1 (CTIP1) is a sequence-specific DNA binding protein. Biochem. J. *368*, 555–563.

Califano, D., Cho, J.J., Uddin, M.N., Lorentsen, K.J., Yang, Q., Bhandoola, A., Li, H., and Avram, D. (2015). Transcription factor Bcl11b controls identity and function of mature type 2 innate lymphoid cells. Immunity *43*, 354–368.

Califano, D., Sweeney, K.J., Le, H., VanValkenburgh, J., Yager, E., O'Connor, W., Kennedy, J.S., Jones, D.M., and Avram, D. (2014). Diverting T helper cell trafficking through increased plasticity attenuates autoimmune encephalomyelitis. J. Clin. Invest. *124*, 174–187.

Chen, Z., Wang, H., D'Souza, C., Sun, S., Kostenko, L., Eckle, S.B., Meehan, B.S., Jackson, D.C., Strugnell, R.A., Cao, H., et al. (2017). Mucosal-associated invariant T-cell activation and accumulation after in vivo infection depends on microbial riboflavin synthesis and co-stimulatory signals. Mucosal Immunol. *10*, 58–68.

Ciofani, M., Madar, A., Galan, C., Sellars, M., Mace, K., Pauli, F., Agarwal, A., Huang, W., Parkurst, C.N., Muratet, M., et al. (2012). A validated regulatory network for Th17 cell specification. Cell *151*, 289–303.

Constantinides, M.G., Link, V.M., Tamoutounour, S., Wong, A.C., Perez-Chaparro, P.J., Han, S.J., Chen, Y.E., Li, K., Farhat, S., Weckel, A., et al. (2019). MAIT cells are imprinted by the microbiota in early life and promote tissue repair. Science *366*, eaax6624.

Corbett, A.J., Eckle, S.B., Birkinshaw, R.W., Liu, L., Patel, O., Mahony, J., Chen, Z., Reantragoon, R., Meehan, B., Cao, H., et al. (2014). T-cell activation by transitory neo-antigens derived from distinct microbial pathways. Nature *509*, 361–365.

Cui, Y., Franciszkiewicz, K., Mburu, Y.K., Mondot, S., Le Bourhis, L., Premel, V., Martin, E., Kachaner, A., Duban, L., Ingersoll, M.A., et al. (2015). Mucosal-associated invariant T cell-rich congenic mouse strain allows functional evaluation. J. Clin. Invest. *125*, 4171–4185.

Dias, J., Boulouis, C., Gorin, J.B., van den Biggelaar, R., Lal, K.G., Gibbs, A., Loh, L., Gulam, M.Y., Sia, W.R., Bari, S., et al. (2018). The CD4(-)CD8(-) MAIT cell subpopulation is a functionally distinct subset developmentally related to the main CD8(+) MAIT cell pool. Proc. Natl. Acad. Sci. U S A *115*, E11513–E11522.

Dolens, A.C., Durinck, K., Lavaert, M., Van der Meulen, J., Velghe, I., De Medts, J., Weening, K., Roels, J., De Mulder, K., Volders, P.J., et al. (2020). Distinct Notch1 and BCL11B requirements mediate human gammadelta/alphabeta T cell development. EMBO Rep. *21*, e49006.

Drashansky, T.T., Helm, E., Huo, Z., Curkovic, N., Kumar, P., Luo, X., Parthasarathy, U., Zuniga, A., Cho, J.J., Lorentsen, K.J., et al. (2019). Bcl11b prevents fatal autoimmunity by promoting Treg cell program and constraining innate lineages in Treg cells. Sci. Adv. *5*, eaaw0480.

Dusseaux, M., Martin, E., Serriari, N., Peguillet, I., Premel, V., Louis, D., Milder, M., Le Bourhis, L., Soudais, C., Treiner, E., and Lantz, O. (2011). Human MAIT cells are xenobiotic-resistant, tissue-targeted, CD161hi IL-17-secreting T cells. Blood *117*, 1250–1259.

Fang, D., Cui, K., Hu, G., Gurram, R.K., Zhong, C., Oler, A.J., Yagi, R., Zhao, M., Sharma, S., Liu, P., et al. (2018). Bcl11b, a novel GATA3-interacting protein, suppresses Th1 while limiting Th2 cell differentiation. J. Exp. Med. *215*, 1449–1462.

Garcia-Perez, L., Famili, F., Cordes, M., Brugman, M., van Eggermond, M., Wu, H., Chouaref, J., Granado, D.S.L., Tiemessen, M.M., Pike-Overzet, K., et al. (2020). Functional definition of a transcription factor hierarchy regulating T cell lineage commitment. Sci. Adv. *6*, eaaw7313.

Gherardin, N.A., Loh, L., Admojo, L., Davenport, A.J., Richardson, K., Rogers, A., Darcy, P.K., Jenkins, M.R., Prince, H.M., Harrison, S.J., et al. (2018). Enumeration, functional responses and cytotoxic capacity of MAIT cells in newly diagnosed and relapsed multiple myeloma. Sci. Rep. *8*, 4159.

Gioulbasani, M., Galaras, A., Grammenoudi, S., Moulos, P., Dent, A.L., Sigvardsson, M., Hatzis, P., Kee, B.L., and Verykokakis, M. (2020). The transcription factor BCL-6 controls early development of innate-like T cells. Nat. Immunol. *21*, 1058–1069.

Godfrey, D.I., Koay, H.F., McCluskey, J., and Gherardin, N.A. (2019). The biology and functional importance of MAIT cells. Nat. Immunol. *20*, 1110–1128.

Gold, M.C., Cerri, S., Smyk-Pearson, S., Cansler, M.E., Vogt, T.M., Delepine, J., Winata, E., Swarbrick, G.M., Chua, W.J., Yu, Y.Y., et al. (2010). Human mucosal associated invariant T cells detect bacterially infected cells. PLoS Biol. *8*, e1000407.

Haddad, E.K., Wu, X., Hammer, J.A., 3rd, and Henkart, P.A. (2001). Defective granule exocytosis in Rab27a-deficient lymphocytes from Ashen mice. J. Cell Biol. *152*, 835–842.

Hasan, S.N., Sharma, A., Ghosh, S., Hong, S.W., Roy-Chowdhuri, S., Im, S.H., Kang, K., and Rudra, D. (2019). Bcl11b prevents catastrophic autoimmunity by controlling multiple aspects of a regulatory T cell gene expression program. Sci. Adv. *5*, eaaw0706.

Holmes, T.D., Vinay Pandey, R., Helm, E.Y., Schlums, H., Han, H., Campbell, T.M., Drashansky, T.T., Chiang, S., Wu, C.-Y., Tao, C., Shoukier, M., et al. (2021). The transcription factor Bcl11b promotes both canonical and adaptive NK cell differentiation. Science Immunology *6* (57), .In press. https://doi.org/10.1126/sciimmunol.abc9801.

Holt, O., Kanno, E., Bossi, G., Booth, S., Daniele, T., Santoro, A., Arico, M., Saegusa, C., Fukuda, M., and Griffiths, G.M. (2008). Slp1 and Slp2-a localize to the plasma membrane of CTL and contribute to secretion from the immunological synapse. Traffic *9*, 446–457.

Hosokawa, H., Romero-Wolf, M., Yang, Q., Motomura, Y., Levanon, D., Groner, Y., Moro, K., Tanaka, T., and Rothenberg, E.V. (2020). Cell type-specific actions of Bcl11b in early T-lineage and group 2 innate lymphoid cells. J. Exp. Med. *217*, e20190972.

Hosokawa, H., Romero-Wolf, M., Yui, M.A., Ungerback, J., Quiloan, M.L.G., Matsumoto, M., Nakayama, K.I., Tanaka, T., and Rothenberg, E.V. (2018). Bcl11b sets pro-T cell fate by site-specific cofactor recruitment and by repressing Id2 and Zbtb16. Nat. Immunol. *19*, 1427–1440.

Kastner, P., Chan, S., Vogel, W.K., Zhang, L.J., Topark-Ngarm, A., Golonzhka, O., Jost, B., Le Gras, S., Gross, M.K., and Leid, M. (2010). Bcl11b represses a mature T-cell gene expression program in immature CD4(+)CD8(+) thymocytes. Eur. J. Immunol. *40*, 2143–2154.

Kjer-Nielsen, L., Patel, O., Corbett, A.J., Le Nours, J., Meehan, B., Liu, L., Bhati, M., Chen, Z., Kostenko, L., Reantragoon, R., et al. (2012). MR1 presents microbial vitamin B metabolites to MAIT cells. Nature *491*, 717–723.

Koay, H.F., Gherardin, N.A., Enders, A., Loh, L., Mackay, L.K., Almeida, C.F., Russ, B.E., Nold-Petry, C.A., Nold, M.F., Bedoui, S., et al. (2016). A three-stage intrathymic development pathway for the mucosal-associated invariant T cell lineage. Nat. Immunol. *17*, 1300–1311.

Koay, H.F., Su, S., Amann-Zalcenstein, D., Daley, S.R., Comerford, I., Miosge, L., Whyte, C.E., Konstantinov, I.E., d'Udekem, Y., Baldwin, T., et al. (2019). A divergent transcriptional landscape underpins the development and functional branching of MAIT cells. Sci. Immunol. *4*, eaay6039.

Kojo, S., Tanaka, H., Endo, T.A., Muroi, S., Liu, Y., Seo, W., Tenno, M., Kakugawa, K., Naoe, Y., Nair, K., et al. (2017). Priming of lineage-specifying genes by Bcl11b is required for lineage choice in post-selection thymocytes. Nat. Commun. *8*, 702.

Kovalovsky, D., Uche, O.U., Eladad, S., Hobbs, R.M., Yi, W., Alonzo, E., Chua, K., Eidson, M., Kim, H.J., Im, J.S., et al. (2008). The BTB-zinc finger transcriptional regulator PLZF controls the development of invariant natural killer T cell effector functions. Nat. Immunol. *9*, 1055–1064.

Kurioka, A., Ussher, J.E., Cosgrove, C., Clough, C., Fergusson, J.R., Smith, K., Kang, Y.H., Walker, L.J., Hansen, T.H., Willberg, C.B., and Klenerman, P. (2015). MAIT cells are licensed through granzyme exchange to kill bacterially sensitized targets. Mucosal Immunol. *8*, 429–440.

Kwong, J., Roundabush, F.L., Hutton Moore, P., Montague, M., Oldham, W., Li, Y., Chin, L.S., and Li, L. (2000). Hrs interacts with SNAP-25 and regulates Ca(2+)-dependent exocytosis. J. Cell Sci. *113*, 2273–2284.

Le Bourhis, L., Dusseaux, M., Bohineust, A., Bessoles, S., Martin, E., Premel, V., Core, M., Sleurs, D., Serriari, N.E., Treiner, E., et al. (2013). MAIT cells detect and efficiently lyse bacterially-infected epithelial cells. PLoS Pathog. *9*, e1003681.

Le Bourhis, L., Martin, E., Peguillet, I., Guihot, A., Froux, N., Core, M., Levy, E., Dusseaux, M., Meyssonnier, V., Premel, V., et al. (2010). Antimicrobial activity of mucosal-associated invariant T cells. Nat. Immunol. *11*, 701–708.

Lee, Y.J., Holzapfel, K.L., Zhu, J., Jameson, S.C., and Hogquist, K.A. (2013). Steady-state production of IL-4 modulates immunity in mouse strains and is determined by lineage diversity of iNKT cells. Nat. Immunol. *14*, 1146–1154.

Legoux, F., Bellet, D., Daviaud, C., El Morr, Y., Darbois, A., Niort, K., Procopio, E., Salou, M., Gilet, J., Ryffel, B., et al. (2019a). Microbial metabolites control the thymic development of mucosal-associated invariant T cells. Science *366*, 494–499.

Legoux, F., Gilet, J., Procopio, E., Echasserieau, K., Bernardeau, K., and Lantz, O. (2019b). Molecular mechanisms of lineage decisions in metabolite-specific T cells. Nat. Immunol. *20*, 1244–1255.

Li, L., Leid, M., and Rothenberg, E.V. (2010a). An early T cell lineage commitment checkpoint dependent on the transcription factor Bcl11b. Science *329*, 89–93.

Li, P., Burke, S., Wang, J., Chen, X., Ortiz, M., Lee, S.C., Lu, D., Campos, L., Goulding, D., Ng, B.L., et al. (2010b). Reprogramming of T cells to natural killer-like cells upon Bcl11b deletion. Science *329*, 85–89.

Lorentsen, K.J., Cho, J.J., Luo, X., Zuniga, A.N., Urban, J.F., Jr., Zhou, L., Gharaibeh, R., Jobin, C., Kladde, M.P., and Avram, D. (2018). Bcl11b is essential for licensing Th2 differentiation during helminth infection and allergic asthma. Nat. Commun. *9*, 1679.

Martin, E., Treiner, E., Duban, L., Guerri, L., Laude, H., Toly, C., Premel, V., Devys, A., Moura, I.C., Tilloy, F., et al. (2009). Stepwise development of MAIT cells in mouse and human. PLoS Biol. *7*, e54.

Ménasché, G., Ménager, M., Lefebvre, J., Deutsch, E., Athman, R., Lambert, N., Mahlaoui, N., Court, M., Garin, J., Fischer, A., and de Saint Basile, G. (2008). A newly identified isoform of Slp2a associates with Rab27a in cytotoxic T cells and participates to cytotoxic granule secretion. Blood *112*, 5052–5062.

Mielke, L.A., Liao, Y., Clemens, E.B., Firth, M.A., Duckworth, B., Huang, Q., Almeida, F.F., Chopin, M., Koay, H.F., Bell, C.A., et al. (2019). TCF-1 limits the formation of Tc17 cells via repression of the MAF-RORgammat axis. J. Exp. Med. *216*, 1682–1699.

Okada, S., Markle, J.G., Deenick, E.K., Mele, F., Averbuch, D., Lagos, M., Alzahrani, M., Al-Muhsen, S., Halwani, R., Ma, C.S., et al. (2015). IMMUNODEFICIENCIES. Impairment of immunity to Candida and Mycobacterium in humans with bi-allelic RORC mutations. Science *349*, 606–613.

Rahimpour, A., Koay, H.F., Enders, A., Clanchy, R., Eckle, S.B., Meehan, B., Chen, Z., Whittle, B., Liu, L., Fairlie, D.P., et al. (2015). Identification of phenotypically and functionally heterogeneous mouse mucosal-associated invariant T cells using MR1 tetramers. J. Exp. Med. *212*, 1095–1108.

Roels, J., Kuchmiy, A., De Decker, M., Strubbe, S., Lavaert, M., Liang, K.L., Leclercq, G., Vandekerckhove, B., Van Nieuwerburgh, F., Van Vlierberghe, P., and Taghon, T. (2020). Distinct and temporary-restricted epigenetic mechanisms regulate human alphabeta and gammadelta T cell development. Nat. Immunol. *21*, 1280–1292.

Salou, M., Legoux, F., Gilet, J., Darbois, A., du Halgouet, A., Alonso, R., Richer, W., Goubet, A.G., Daviaud, C., Menger, L., et al. (2019). A common transcriptomic program acquired in the thymus defines tissue residency of MAIT and NKT subsets. J. Exp. Med. *216*, 133–151.

Sattler, A., Dang-Heine, C., Reinke, P., and Babel, N. (2015). IL-15 dependent induction of IL-18 secretion as a feedback mechanism controlling human MAIT-cell effector functions. Eur. J. Immunol. *45*, 2286–2298.

Savage, A.K., Constantinides, M.G., Han, J., Picard, D., Martin, E., Li, B., Lantz, O., and Bendelac, A. (2008). The transcription factor PLZF directs the effector program of the NKT cell lineage. Immunity *29*, 391–403.

Slichter, C.K., McDavid, A., Miller, H.W., Finak, G., Seymour, B.J., McNevin, J.P., Diaz, G., Czartoski, J.L., McElrath, M.J., Gottardo, R., and Prlic, M. (2016). Distinct activation thresholds of human conventional and innate-like memory T cells. JCI Insight *1*, e86292.

Stinchcombe, J.C., Barral, D.C., Mules, E.H., Booth, S., Hume, A.N., Machesky, L.M., Seabra, M.C., and Griffiths, G.M. (2001). Rab27a is required for regulated secretion in cytotoxic T lymphocytes. J. Cell Biol. *152*, 825–834.

Tilloy, F., Treiner, E., Park, S.H., Garcia, C., Lemonnier, F., de la Salle, H., Bendelac, A., Bonneville, M., and Lantz, O. (1999). An invariant T cell receptor alpha chain defines a novel TAP-independent major histocompatibility complex class Ib-restricted alpha/beta T cell subpopulation in mammals. J. Exp. Med. *189*, 1907–1921.

Treiner, E., Duban, L., Bahram, S., Radosavljevic, M., Wanner, V., Tilloy, F., Affaticati, P., Gilfillan, S., and Lantz, O. (2003). Selection of evolutionarily conserved mucosal-associated invariant T cells by MR1. Nature *422*, 164–169.

Uddin, M.N., Sultana, D.A., Lorentsen, K.J., Cho, J.J., Kirst, M.E., Brantly, M.L., Califano, D., Sant'Angelo, D.B., and Avram, D. (2016). Transcription factor Bcl11b sustains iNKT1 and iNKT2 cell programs, restricts iNKT17 cell program, and governs iNKT cell survival. Proc. Natl. Acad. Sci. U S A *113*, 7608–7613.

Ussher, J.E., Bilton, M., Attwod, E., Shadwell, J., Richardson, R., de Lara, C., Mettke, E., Kurioka, A., Hansen, T.H., Klenerman, P., and Willberg, C.B. (2014). CD161++ CD8+ T cells, including the MAIT cell subset, are specifically activated by IL-12+IL-18 in a TCR-independent manner. Eur. J. Immunol. *44*, 195–203.

Vacchini, A., Chancellor, A., Spagnuolo, J., Mori, L., and De Libero, G. (2020). MR1-Restricted T cells are unprecedented cancer fighters. Front. Immunol. *11*, 751.

van Wilgenburg, B., Loh, L., Chen, Z., Pediongco, T.J., Wang, H., Shi, M., Zhao, Z., Koutsakos, M., Nussing, S., Sant, S., et al. (2018). MAIT cells contribute to protection against lethal influenza infection in vivo. Nat. Commun. *9*, 4706.

van Wilgenburg, B., Scherwitzl, I., Hutchinson, E.C., Leng, T., Kurioka, A., Kulicke, C., de Lara, C., Cole, S., Vasanawathana, S., Limpitikul, W., et al. (2016). MAIT cells are activated during human viral infections. Nat. Commun. *7*, 11653.

Vanvalkenburgh, J., Albu, D.I., Bapanpally, C., Casanova, S., Califano, D., Jones, D.M., Ignatowicz, L., Kawamoto, S., Fagarasan, S., Jenkins, N.A., et al. (2011). Critical role of Bcl11b in suppressor function of T regulatory cells and prevention of inflammatory bowel disease. J. Exp. Med. *208*, 2069–2081.

Wakabayashi, Y., Watanabe, H., Inoue, J., Takeda, N., Sakata, J., Mishima, Y., Hitomi, J., Yamamoto, T., Utsuyama, M., Niwa, O., et al. (2003). Bcl11b is required for differentiation and survival of alphabeta T lymphocytes. Nat. Immunol. *4*, 533–539.

Walker, J.A., Oliphant, C.J., Englezakis, A., Yu, Y., Clare, S., Rodewald, H.R., Belz, G., Liu, P., Fallon, P.G., and McKenzie, A.N. (2015). Bcl11b is essential for group 2 innate lymphoid cell development. J. Exp. Med. *212*, 875–882.

Wang, H., Kjer-Nielsen, L., Shi, M., D'Souza, C., Pediongco, T.J., Cao, H., Kostenko, L., Lim, X.Y., Eckle, S.B.G., Meehan, B.S., et al. (2019). IL-23 costimulates antigen-specific MAIT cell activation and enables vaccination against bacterial infection. Sci. Immunol. *4*, eaaw0402.

Yu, Y., Wang, C., Clare, S., Wang, J., Lee, S.C., Brandt, C., Burke, S., Lu, L., He, D., Jenkins, N.A., et al. (2015). The transcription factor Bcl11b is specifically expressed in group 2 innate lymphoid cells and is essential for their development. J. Exp. Med. *212*, 865–874.

Zhang, S., Laouar, A., Denzin, L.K., and Sant'Angelo, D.B. (2015). Zbtb16 (PLZF) is stably suppressed and not inducible in non-innate T cells via T cell receptor-mediated signaling. Sci. Rep. *5*, 12113.

Zhang, S., Rozell, M., Verma, R.K., Albu, D.I., Califano, D., Vanvalkenburgh, J., Merchant, A., Rangel-Moreno, J., Randall, T.D., Jenkins, N.A., et al. (2010). Antigen-specific clonal expansion and cytolytic effector function of CD8+ T lymphocytes depend on the transcription factor Bcl11b. J. Exp. Med. *207*, 1687–1699.

iScience, Volume *24*

Supplemental information

BCL11B is positioned upstream of PLZF and RORγt to control thymic development of mucosal-associated invariant T cells and MAIT17 program

Theodore T. Drashansky, Eric Y. Helm, Nina Curkovic, Jaimee Cooper, Pingyan Cheng, Xianghong Chen, Namrata Gautam, Lingsong Meng, Alexander J. Kwiatkowski, William O. Collins, Benjamin G. Keselowsky, Derek Sant'Angelo, Zhiguang Huo, Weizhou Zhang, Liang Zhou, and Dorina Avram

Supplementary Information

Supplementary Figures

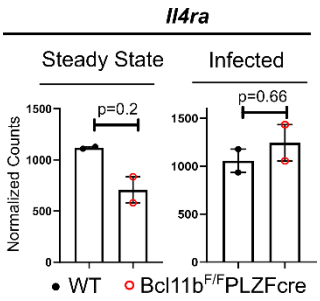

Figure S1, related to Figure 2. I*L4Ra* mRNA levels are high in MAIT cells and not altered by Bcl11b removal. DESeq2 normalized counts for *IL4Ra* in Bcl11b KO and WT MAIT cells in lung at steady state or following *Salmonella* infection. RNA-seq was performed on sorted lin- TCRβ +MR1t-5-OP-RU+ MAIT cells from lung of Bcl11b$^{F/F}$PLZFcre/R26R-EYFP mice and WT control mice at steady state or infected with *Salmonella* Typhimurium BRD509 (*Salmonella*) intranasally, day 7 post infection. For Bcl11b$^{F/F}$ PLZFcre/R26R-EYFP mice, in addition to lin- TCRβ + MR1t-5-OP-RU+, sorting was conducted on YFP+ cells. Additional details are provided in Fig. 5 and Material and Methods. False discovery rate (FDR)–adjusted *p* values were calculated using the Benjamini-Hochberg method with a significance cutoff of adjusted $p < 0.05$.

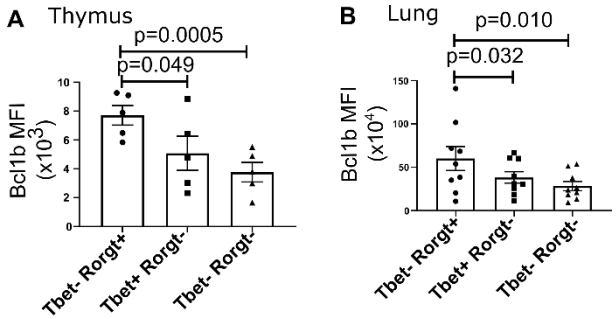

Figure S2, related to Figure 3. Bcl11b levels in MAIT functional subsets. (**A** and **B**) Bcl11b MFI in MAIT1, MAIT17 and double negative WT MAIT cells in the thymus (**A**) and lungs (**B**) of

uninfected mice. Student's t-test was used for statistical analysis. $p < 0.05$ was considered significant.

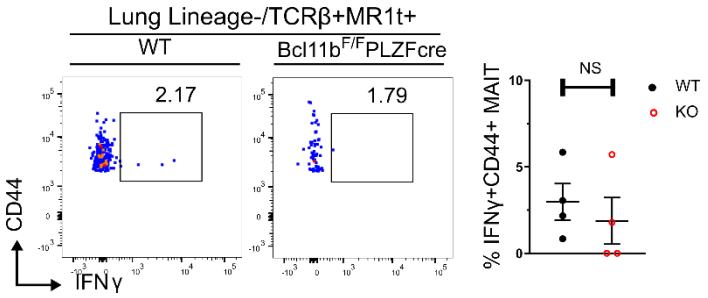

Figure S3, related to Figure 3. IFNγ levels are low and equal in Bcl11b KO and WT MAIT cells at steady state. Representative dot plots (left) and frequencies (right) of Bcl11b KO and WT IFNγ+CD44+ MR1t-5-OP-RU+ TCRβ lin- MAIT cells in lung at steady state. Each point represents a concatenated file of 2 lung samples run independently. Statistics were conducted as paired t-test. $p < 0.05$ was considered significant.

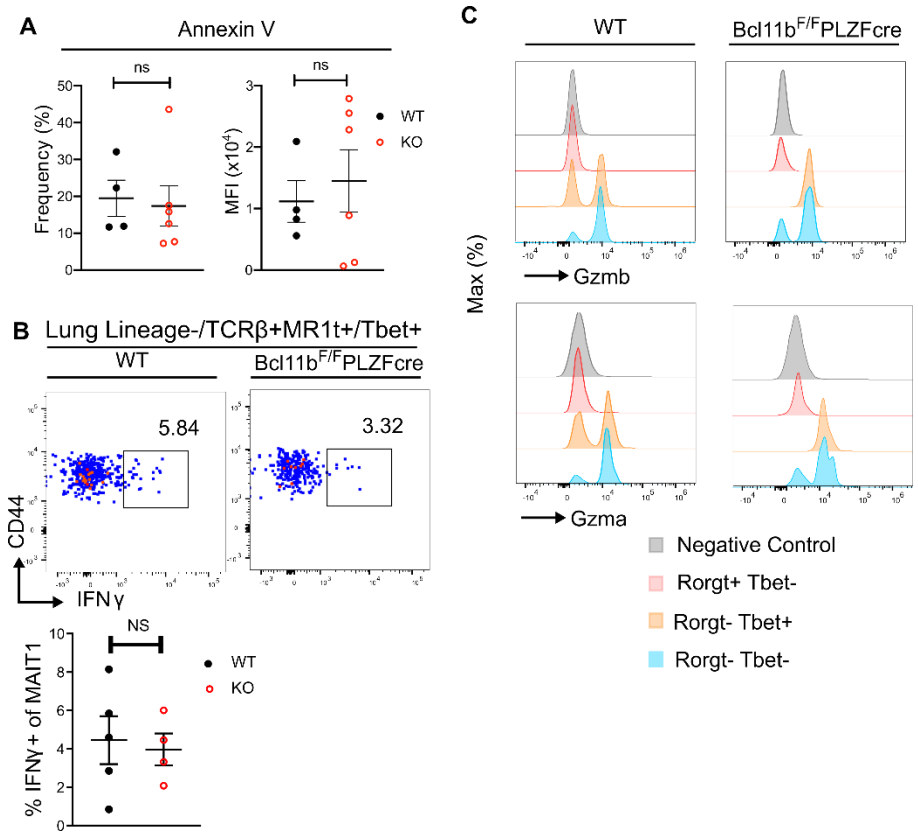

Figure S4, related to Figure 4. Analysis of Bcl11b KO and WT MAIT cells following *Salmonella* BRD509 infection. Bcl11b$^{F/F}$ PLZFcre and WT mice were infected with *Salmonella* BRD509 intranasally and euthanized 7 days post infection. (**A**) Frequencies and MFI of Annexin V staining of Bcl11b KO and WT MR1t-5-OP-RU+ MAIT cells in the lung following *Salmonella* infection. (**B**) Representative dot plots and frequencies of IFNγ+CD44+ MR1t-5-OP-RU+ MAIT cells following *Salmonella* infection. (**C**) Representative histograms of GzmB and GzmA staining in Bcl11b KO and WT MAIT17, MAIT1 and Rorγt-Tbet- MR1t-5-OP-RU+ MAIT cells in the lung of infected mice. Negative control represents gated lineage+ TCRβ- cells. Statistics were conducted as paired t-test. $p < 0.05$ was considered significant.

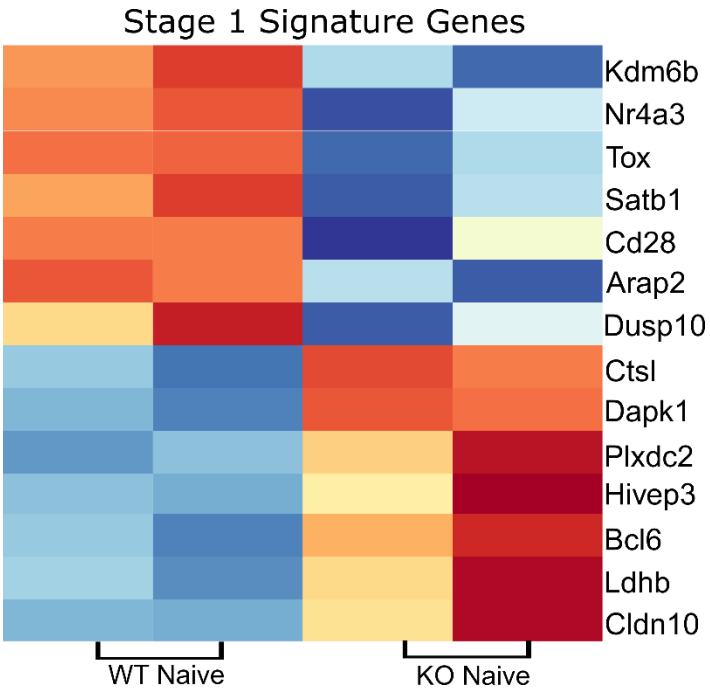

Figure S5, related to Figure 5. Stage 1 signature genes in lung MAIT cells in the absence of Bcl11b. RNA-seq was performed on sorted lin- TCRβ + MR1t-5-OP-RU+ MAIT cells from lung of Bcl11b$^{F/F}$PLZFcre/R26R-EYFP mice and WT control mice at steady state. For Bcl11b$^{F/F}$ PLZFcre/R26R-EYFP mice, in addition to TCRβ +MR1t+, sorting was conducted on YFP+ cells. Heatmaps of differentially expressed stage 1 genes in lung Bcl11b KO and WT MR1t-5-OP-RU+ MAIT cells at steady state.

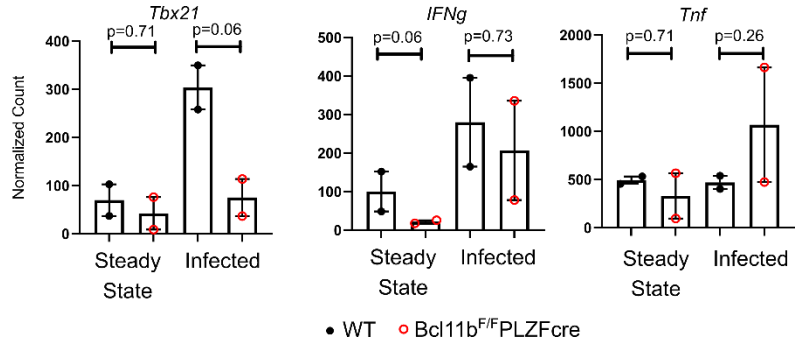

Figure S6, related to Figure 5. MAIT1 genes are not significantly altered in the absence of Bcl11b at steady state or following infection. DESeq2 normalized counts for *Tbx21, Ifn*γ and *Tnf* in Bcl11b KO and WT MAIT cells in lung at steady state or following *Salmonella* infection. RNA-seq was performed on sorted lin- TCRβ +MR1t-5-OP-RU+ MAIT cells from lung of Bcl11b$^{F/F}$PLZFcre/R26R-EYFP mice and WT control mice at steady state or infected with *Salmonella* Typhimurium BRD509 (*Salmonella*) intranasally, day 7 post infection. For Bcl11b$^{F/F}$ PLZFcre/R26R-EYFP mice, in addition to lin- TCRβ+ MR1t-5-OP-RU+, sorting was conducted on YFP+ cells. Additional details are provided in Fig. 5 and Material and Methods. False discovery rate (FDR)–adjusted *p* values were calculated using the Benjamini-Hochberg method, with a significance cutoff of adjusted $p < 0.05$.

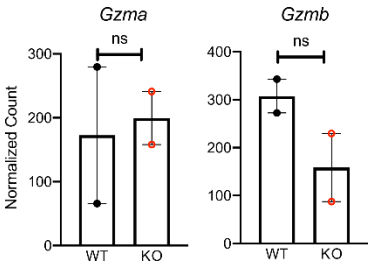

Figure S7, related to Figure 5. Granzyme mRNAs are unaffected by Bcl11b deletion in MAIT cells. DESeq2 normalized counts for *Gzma* and *Gzmb* in lung of Bcl11b KO and WT

MAIT cells from *Salmonella* infected mice. RNA-seq was performed on sorted lin- TCRβ +MR1t-5-OP-RU+ MAIT cells from lung of Bcl11b$^{F/F}$PLZFcre/R26R-EYFP mice and WT control mice at steady state or infected with *Salmonella* Typhimurium BRD509 (*Salmonella*) intranasally, day 7 post infection. For Bcl11b$^{F/F}$ PLZFcre/R26R-EYFP mice, in addition to lin- TCRβ + MR1t-5-OP-RU+, sorting was conducted on YFP+ cells. Additional details are provided in Fig. 5 and Material and Methods. False discovery rate (FDR)–adjusted *p* values were calculated using the Benjamini-Hochberg method, with a significance cutoff of adjusted $p < 0.05$.

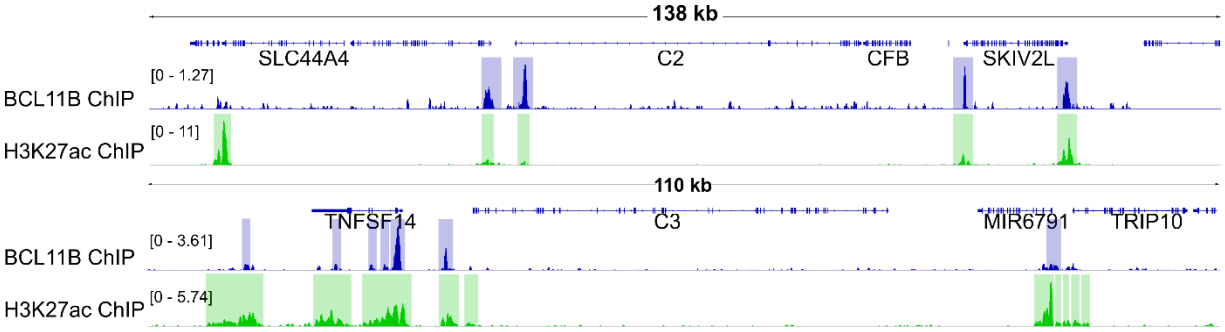

Figure S8, related to Figure 8. Bcl11b binding ant H3K27Ac at *C2* and *C3* complement loci in human MAIT cells from healthy donors. IGV visualization of *C2* and *C3* loci from Bcl11b ChIP-seq (track 1) and H3K27Ac (track 2) human MAIT cells. Blue and green highlights indicate significant ChIP-seq peaks. ChIP-seq scale bar normalized to sequences per million reads.

Table S3. MAIT17 program genes and differential expression at steady state or infection (compiled from Koay et al. 2019), **related to Figure 5**.

Genes	**DEG in Bcl11b KO versus WT - steady state**	**DEG in Bcl11b KO versus WT - infection**
Blk	down	down
Pxdc1	down	down
S100a4	down	down
Actn2	down	down
Aqp3	down	NC
Cd7	down	NC
Apol7b	down	down
Tnfrsf25	down	down
Stab2	down	NC
Emb	down	down
Sdc1	down	NC
Itgae	down	down
Ramp1	down	down
Ramp3	down	down
Icos	down	down
Il27ra	down	down
Il12rb	down	down
Cd44	down	down
Ccr2	down	down
Zbtb16	down	down
Maf	down	down
Il7r	down	down
Il18r1	down	down
Il17a	down	down
Il23r	down	down

Il17rb	down	down
Il1r1	down	down
Il17re	down	down
Rorc	down	down
Ccr6	down	down
Tmem176a	NC	NC
Serpinb1a	NC	down
Tmem176b	NC	NC
Lrrc17	NC	NC
Lrrc58	NC	NC
Cabin1	NC	down
Chad	NC	NC
Kcnk1	NC	NC
Avpi1	NC	NC
Prelid1	NC	NC
Jag1	NC	up
Mycn	NC	NC
Rnf208	NC	down
Il17f	NC	down
Il22	NC	NC
Cxcl2	NC	up
Iltifb	NC	NC

Table S4. MAIT1 program genes and differential expression at steady state or infection (compiled from Koay et al. 2019), **related to Figure 5**.

Genes	**DEG in Bcl11b KO versus WT - steady state**	**DEG in Bcl11b KO versus WT - infection**
Klrk1	NC	NC
Fgl2	down	NC
Cd28	down	down
Il2rb	down	down
Satb1	down	NC
Nkg7	NC	NC
Klrd1	NC	NC
Ly6c2	NC	up
Klrb1c	NC	NC
Gzmb	NC	NC
Gimap3	NC	NC
Klra3	NC	NC
Ms4a4b	NC	NC
Klra9	NC	NC
AW112010	NC	NC
Slamf7	NC	up
Klrc2	NC	NC
Hsd11b1	NC	NC
H2-Q6	NC	NC
Stat4	NC	down
Klra5	NC	NC
Klrc1	NC	NC
Styk1	NC	NC
Klra13-ps	NC	NC
Itga4	NC	NC

H2-K1	NC	NC
Klra6	NC	NC
Klra8	NC	NC
Klra10	NC	NC
Klrc2	NC	NC
Klre	NC	NC
Ugcg	NC	NC
Inpp4b	NC	NC
Bcl2	NC	NC
Itm2a	NC	NC
Ccl5	NC	NC
Ifng	NC	NC
Il21r	NC	NC
Xcl1	NC	NC
Cxcr3	NC	down
Ccl4	NC	up
Ccr9	NC	NC
Ccl3	NC	up
Lef1	NC	NC
Il10ra	NC	up
Il18rap	NC	NC
Cxcr4	NC	NC

Table S5. CD4+Lef1+CD138-CD319- early stage 3 precursor program genes and differential expression at steady state or infection (compiled from Koay et al. 2019), **related to Figure 5**.

Genes	DEG in Bcl11b KO versus WT - steady state	DEG in Bcl11b KO versus WT - infection
Satb1	down	NC
Tcf7	down	down
Cd4	NC	up
Lef1	NC	NC
Itm2a	NC	NC
Cd27	NC	NC

Table S6. TCR Signaling pathway genes and differential expression at steady state or infection, related to Figure 5.

Genes	DEG in Bcl11b KO versus WT - steady state	DEG in Bcl11b KO versus WT - infection
Pdpk1	NC	NC
Bcl10	NC	NC
Cd247	NC	NC
Cd28	down	down
Cd3d	down	Down
Cd3e	down	Down
Cd3g	down	Down
Cd4	NC	up
Cd40l	down	down
Cd8a	NC	NC
Cd8b1	NC	NC
Fos	NC	NC
Fyn	NC	down
Grap2	down	down
Hras	NC	NC
Itk	down	down
Kras	NC	NC
Malt1	NC	up
Rasgrp1	down	Down
4930544G11Rik	NC	NC
Card11	down	Down
Cdc42	NC	NC
Csf2	NC	NC
Chuk	NC	NC
Cdk4	NC	NC
Ctla4	NC	down
Dlg1	NC	NC
Gsk3b	NC	NC

Grb2	NC	NC
Icos	down	down
Ikbkb	NC	NC
Ikbkg	NC	NC
Ifng	NC	NC
Jun	NC	NC
Lat	down	down
Lck	down	down
Mapk1	NC	NC
Mapk11	NC	NC
Mapk12	NC	NC
Mapk13	up	NC
Mapk14	NC	NC
Mapk3	NC	NC
Map2k1	NC	NC
Map2k2	NC	NC
Map2k7	NC	NC
Map3k14	down	down
Map3k7	NC	NC
Map3k8	NC	NC
Nras	NC	NC
Nck1	NC	NC
Nck2	NC	NC
Nfatc1	down	Down
Nfatc2	NC	Down
Nfatc3	down	down
Nfkb1	NC	NC
Nfkbia	NC	NC
Nfkbib	NC	NC
Nfkbie	Down	NC
Pak1	NC	up
Pak2	NC	NC
Pak3	NC	NC
Pak4	NC	NC
Pak5	NC	NC
Pak6	NC	NC
Pak7	NC	NC
Pik3r3	NC	NC
Pik3cd	down	NC
Pik3ca	NC	NC
Pik3cb	NC	up
Pik3r1	NC	NC
Pik3r2	NC	Up
Pik3cg	down	NC
Pik3r5	NC	NC
Plcg1	NC	down
Pdcd1	down	down
Ppp3ca	NC	NC
Ppp3cb	NC	down

Ppp3cc	NC	NC
Ppp3r1	NC	NC
Ppp3r2	NC	NC
Ptpn6	NC	NC
Ptprc	down	NC
Rhoa	NC	NC
Sos1	NC	NC
Sos2	NC	NC
Tec	NC	NC
Raf1	NC	NC
Rela	NC	NC
Vav1	NC	NC
Vav2	NC	NC
Vav3	NC	up
Zap70	down	down

Table S7. Key Resources Table. Antibodies.

Antibody	SOURCE	IDENTIFIER
Anti-mouse T-bet, BV421	Biolegend	Cat #: 644816
Anti-mouse granzyme A, eFluor450	eBioscience	Cat #: 48-4831-82
Anti-mouse CD45.2 eFluor506	eBioscience	Cat #: 69-0454-82
Anti-mouse CD44, BV510	Biolegend	Cat #: 103044
Anti-mouse TCRβ, Super Bright 600	eBioscience	Cat #: 63-5961-82
Anti-mouse B220, BV650	Biolegend	Cat #: 103241
Anti-mouse CD11c, BV650	Biolegend	Cat #: 117339
Anti-mouse GR1, BV650	Biolegend	Cat #: 108442
Anit-mouse CD45.1, Super Bright 702	eBioscience	Cat #: 67-0453-82
Anti-mouse TNF, BV750	Biolegend	Cat #: 506358
Anti-mouse IFNγ, BV785	Biolegend	Cat #: 17-6988-82
Anti-mouse MR1-5-OP-RU, PE or APC	NTCF	N/A
Anti-mouse MR1-6-FP, PE or APC	NTCF	N/A
Anti-mouse granzyme B, PE/CF594	BD Biosciences	Cat #: 562462
Anti-mouse IL-17A, PE/cy7	eBioscience	Cat #: 25-7177-82
Anti-mouse/human Bcl11b, rabbit	Bethyl Labs	Cat #: A300-385A
Goat-anti-rabbit secondary, AlexaFluor488	ThermoFisher	Cat #: A11008
Anti-mouse PLZF, PerCP/cy5.5	Biolegend	Cat #: 145808
Anti-mouse Rorγt, APC	eBioscience	Cat #: 17-6988-82

Fixable viability dye, eFluor780	eBioscience	Cat #: 65-0865-14
Anti-mouse CD8a, Super Bright 702	eBioscience	Cat #: 67-0081-82
Anti-mouse Ki67, AlexFluor700	Biolegend	Cat #: 652420
Annexin V, Pacific Blue	eBioscience	Cat #: 640918
Anti-human CD3, PerCP/cy5.5	Biolegend	Cat #: 317338
Anti-human CD161, PE/Texas Red	Biolegend	Cat #: 339940
Anti-human TCRVα7.2, BV421	Biolegend	Cat #: 351716
Anti-human CD4, Biotin	Biolegend	Cat #: 317438
Anti-human CD11b, Biotin	Biolegend	Cat #: 301304
Anti-human CD14, Biotin	Biolegend	Cat #: 301826
Anti-mouse T-bet, PE/cy7	eBioscience	Cat #: 25-5825-82
Anti-mouse CD24, BV605	Biolegend	Cat #: 101827
Anti-mouse CD69, PerCP/cy5.5	Biolegend	Cat #: 104522
Anti-mouse CD8a, BV785	Biolegend	Cat #: 100750
Anti-mouse CD44, APC/cy7	Biolegend	Cat #: 103028
Anti-mouse TCRβ, eFluor450	eBioscience	Cat #: 48-5961-82
Anti-mouse CD62L, BV711	Biolegend	Cat #: 104445
Anti-Streptavidin, PE	Agilent	Cat #: PJRS25

Transparent Methods

Mice. PLZFcre^{+} mice (Zhang et al. 2015) were bred with Bcl11b$^{F/F}$ mice, on a C57BL/6 background, to generate Bcl11b$^{F/F}$ PLZFcre+ (KO) and Bcl11b$^{F/F}$ (WT) mice and further with R26R-EYFP mice to generate Bcl11b$^{F/F}$ PLZFcre/R26R-EYFP mice. Both males and females of 6-8 weeks of age were used in all experiments conducted. Littermates of the same sex were used, as WT and KO mice. Mice were bred and maintained under specific pathogen-free conditions and kept in-house for experiments in individually ventilated cages under specific pathogen-free conditions. All experiments were conducted according to animal protocols approved by Institutional Animal Care and Use Committees of University of Florida, Moffitt Cancer Center and University of South Florida.

Salmonella Typhimurium BRD509 Infections. *Salmonella enterica* ser. Typhimurium BRD509 was provided by Dr. Stephen J. McSorley of UC- Davis. 10^6 cfu of *Salmonella* was instilled intra-nasally and mice were euthanized after 7 days.

Human Subjects. PBMCs derived buffy coats of healthy volunteers were purchased from LifeSouth Community Blood Centers. MAIT cells were sorted as CD3+CD161+TCRVα7.2+ cells.

Bone Marrow Chimeras. Cells were isolated from bone marrows (BM) of $Bcl11b^{F/F}$ PLZF-Cre^{+} (KO) (CD45.2) and WT (CD45.1/2) mice and mixed at a 1:1 ratio. 10 million BM cells were injected i.v. into lethally irradiated CD45.1 recipient mice. Prior to transfer CD45.1 mice were irradiated 2 times, 4 hours apart with 550 rad. Mice were analyzed 8 weeks post-transplant.

MR1 tetramer. Biotinylated MR1-5-OP-RU and MR1-6-FP monomers were obtained from the National Institutes of Health Tetramer Core Facility and were tetramerized with Strepavidin-PE or -APC. Tetramer was titrated on WT MAIT cells form thymus and lung.

Cell Isolation and analysis. Cell isolation was performed as previously described by VanValkenburgh *et al.*(Vanvalkenburgh et al. 2011). Briefly, cells from all lymphoid organs were placed on 40 µm filter and pressed through the filter while washed with 1% FBS complete RPMI medium. Lungs were processed using the gentleMACS Dissociator in 1% FBS complete RPMI medium with 10mg/mL of Collagenase A and 5µg/mL of DNAse I with the protocol for setting Lung 1, followed by for 30 minutes incubation at 37C with shaking at 220rpm. Digestion was stopped with 50 µL of 0.5M of EDTA. and further Lung setting 2 protocol was conducted. Tissue was passed through 40 µm filter and washed with additional 1% FBS complete RPMI medium, centrifuged at 350 *x g* for 10 minutes. The pellets were resuspended in 30% Percoll and layered on top of 70% Percoll and centrifuged at 2500rpm for 20 minutes. For analysis of cytokine production, cells were resuspended in 10% complete RPMI media at a concentration of 1 x 10^8

cells/ml in the presence of PMA and ionomycin, at a final concentration of 25ng/ml and 1µg/mL, respectively for 5 hours with Brefeldin A added to a final concentration of 0.3µM, for the last 4 hours.

For thymic MAIT cells only, a CD8+ T cell negative selection enrichment kit was used in total thymocytes, given that in the thymus MAIT cells are rarely CD4+ or DP.

For the lung cells, no enrichment was used, however cells were stained with a cocktail of B220, Gr1, Cd11b (all PE-Cy7) (dump gate, (lin+)), as well as for TCRβ and with MR1t-5-OP-RU. TCRβ and with MR1t-5-OP-RU+ cells were analyzed in the lin- population.

Antibodies and fluorophores information is provided in Table S7.

RNA-seq library preparation. RNA was extracted from sort-purified WT and Bcl11b KO (YFP+) lin- TCRβ + MR1t-5-OP-RU+ MAIT cells from *Salmonella* BRD509 infected or unifected $Bcl11b^{F/F}$ (WT) and $Bcl11b^{F/F}$ $PLZFcre^{+}$ $Rosa26YFP^{+}$ mice, using the RNeasy Plus Micro Kit (QIAGEN 74034), and rRNA was depleted using NEBNext rRNA Depletion Kit (NEB E63102). cDNA libraries were prepared using NEBNext Ultra II RNA Library Prep Kit (NEB E7770S), quality was assessed on a Bioanalyzer (Agilent, #5067-4626), and sequenced on a HiSeq3000 at approximately 30 million reads per library.

BCL11B ChIP-seq. Human MAIT cells were sort purified from PBMCs as CD3+CD161+TCRVα7.2+ cells derived from nine donors. ChIP-Seq against Bcl11b was performed on MAIT cells using the SimpleChIP Enzymatic Chromatin IP Kit from Cell Signaling Technologies (CST #9003), following their recommended protocol up to the library preparation with the following alterations: (1) 10^7 cells were used in place of 4×10^7; (2) formaldehyde fixation was performed in 1 mL; (3) Buffer A and Buffer B steps were performed in 1 mL; (4) cells were sheared in ChIP-buffer to an average of 200-1000bp using a Diagenode Bioruptor Pico (Diagenode B01060002); (5) a cocktail of 3 anti-Bcl11b antibodies

were used (8mg ab18465, 8 mg of CST #12120 and 8mg of Bethyl A300-385 per ChIP); (6) final DNA purification was performed by phenol:chloroform:isoamyl alcohol extraction with MaXtract high density columns (Qiagen #129046). Libraries were prepared using NEBNext Ultra II DNA Library Prep Kit (NEB #E7645S) and sequenced as PE 2x100 on a HiSeq3000.

H3K27ac ChIP-seq. ChIP-seq for H3K27ac was performed on two independent samples derived from two donors. 100,000 sort purified human MAIT cells (CD3+CD161+TCRVα7.2+ using the Low Cell ChIP-Seq kit from Active Motif (#104895) following strictly the manufacturer's recommended protocol scaled to 100,000 cells. H3K27ac antibody was from Cell Signaling Technologies (#8173) at the recommended 1:100 dilution. Libraries were run as PE 2x100 on a HiSeq3000.

QUANTIFICATION AND STATISTICAL ANALYSIS

RNA-seq Data Processing. RNA-seq fastq files were trimmed using seqtk and the quality assessed using FastQC (Lorentsen et al. 2018). The trimmed reads were aligned to the mouse genome (mm10) using Hisat2 and transcript counts were obtained using HTseq (Lorentsen et al. 2018). DeSeq2 was used for differential expression analysis (Lorentsen et al. 2018). Significance for RNA-seq data was determined using DeSeq2 (Love, Huber and Anders 2014).

ChIP-seq data Processing. Data analysis for ChIP-seq was performed using a customized pipeline based on a previously published version (Lorentsen et al. 2018). Briefly, fastq files were first trimmed using Trimmomatic and read quality was assessed using FastQC. Reads were aligned to the mouse genome (mm10) using Bowtie2. The resulting SAM file was pruned (Q>30), converted to BAM format and was sorted using SAMtools. Duplicate reads were removed using Picard tools and MACS2 was used for peak calling and bedgraph file preparation. Bedgraph files were visualized using Integrative Genomics Viewer (IGV).

Statistics. For the Spearman Correlation plot, tag counts of each peak in Bcl11b and H3K27ac and peak annotation were obtained using HOMER software. Correlation in the tag counts

between Bcl11b and H3K27ac was evaluated using the Spearman's method. P-value was obtained from Student's t-test to examine if the correlation was significant and analysis was carried out in R. For all mouse experiments where the mice were not infected with *Salmonella* BRD509, two files were concatenated to create individual points on the frequency statistics graphs and for representative figures. For all flow cytometry experiments data was analyzed in GraphPad Prism. For single comparisons, we used two-tailed Student's *t*-test, and $p<0.05$ were considered significant. In case of multiple groups of mice of different phenotypes, we used an analysis of variance or a Kruskal-Wallis test applicable for continuous variables.

References

Koay, H. F., S. Su, D. Amann-Zalcenstein, S. R. Daley, I. Comerford, L. Miosge, C. E. Whyte, I. E. Konstantinov, Y. d'Udekem, T. Baldwin, P. F. Hickey, S. P. Berzins, J. Y. W. Mak, Y. Sontani, C. M. Roots, T. Sidwell, A. Kallies, Z. Chen, S. Nussing, K. Kedzierska, L. K. Mackay, S. R. McColl, E. K. Deenick, D. P. Fairlie, J. McCluskey, C. C. Goodnow, M. E. Ritchie, G. T. Belz, S. H. Naik, D. G. Pellicci & D. I. Godfrey (2019) A divergent transcriptional landscape underpins the development and functional branching of MAIT cells. *Sci Immunol,* 4 (41):eaay6039

Vanvalkenburgh, J., D. I. Albu, C. Bapanpally, S. Casanova, D. Califano, D. M. Jones, L. Ignatowicz, S. Kawamoto, S. Fagarasan, N. A. Jenkins, N. G. Copeland, P. Liu & D. Avram (2011) Critical role of Bcl11b in suppressor function of T regulatory cells and prevention of inflammatory bowel disease. *J Exp Med,* 208**,** 2069-81.

Koay, H. F., S. Su, D. Amann-Zalcenstein, S. R. Daley, I. Comerford, L. Miosge, C. E. Whyte, I. E. Konstantinov, Y. d'Udekem, T. Baldwin, P. F. Hickey, S. P. Berzins, J. Y. W. Mak, Y. Sontani, C. M. Roots, T. Sidwell, A. Kallies, Z. Chen, S. Nussing, K. Kedzierska, L. K. Mackay, S. R. McColl, E. K. Deenick, D. P. Fairlie, J. McCluskey, C. C. Goodnow, M. E. Ritchie, G. T. Belz, S. H. Naik, D. G. Pellicci & D. I. Godfrey (2019) A divergent transcriptional landscape underpins the development and functional branching of MAIT cells. *Sci Immunol,* 4.

Lorentsen, K. J., J. J. Cho, X. Luo, A. N. Zuniga, J. F. Urban, Jr., L. Zhou, R. Gharaibeh, C. Jobin, M. P. Kladde & D. Avram (2018) Bcl11b is essential for licensing Th2 differentiation during helminth infection and allergic asthma. *Nat Commun,* 9**,** 1679.

Love, M. I., W. Huber & S. Anders (2014) Moderated estimation of fold change and dispersion for RNA-seq data with DESeq2. *Genome Biology,* 15**,** 550.

Vanvalkenburgh, J., D. I. Albu, C. Bapanpally, S. Casanova, D. Califano, D. M. Jones, L. Ignatowicz, S. Kawamoto, S. Fagarasan, N. A. Jenkins, N. G. Copeland, P. Liu & D. Avram (2011) Critical role of Bcl11b in suppressor function of T regulatory cells and prevention of inflammatory bowel disease. *J Exp Med,* 208**,** 2069-81.

Zhang, S., A. Laouar, L. K. Denzin & D. B. Sant'Angelo (2015) Zbtb16 (PLZF) is stably suppressed and not inducible in non-innate T cells via T cell receptor-mediated signaling. *Sci Rep,* 5**,** 12113.